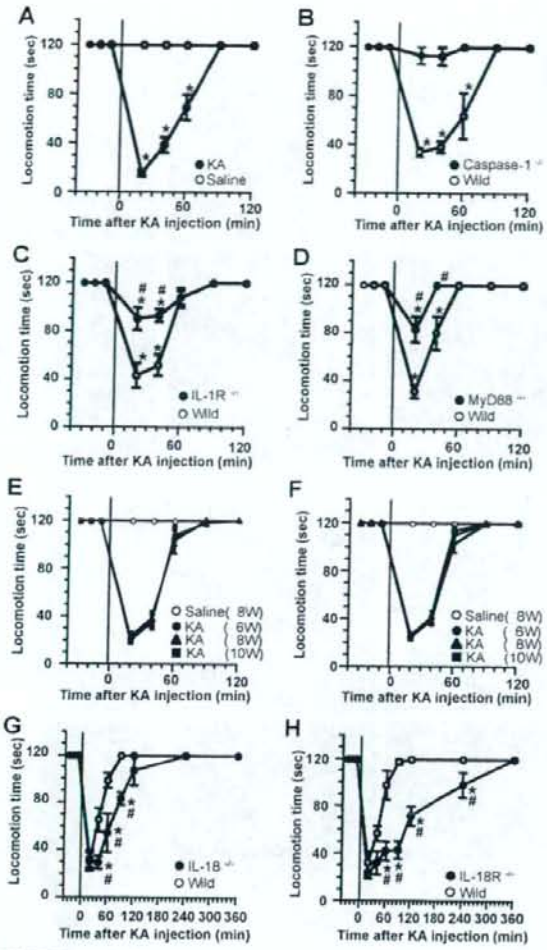

FIGURE 1. Deficiency with caspase-1, IL-1 receptor type I, or MyD88 attenuates the effect of kainate on inducing ataxia, but deficiency with IL-18 or its receptor delay the recovery from kainate-induced ataxia. *A*, Effect of kainate on locomotion activity in normal BALB/c mice was examined. Before kainate administration, a rotarod test was performed every 10 min (three times) and then kainate (KA) (20 mg/kg: F) or saline (E) was i.p. injected into BALB/c mice at time 0. A rotarod test was performed at 20, 40, 60, 90, and 120 min after kainate injection. , p 0.05 when compared with average data before kainate injection (n 5). *B–D*, *G*, and *H*, Effect of kainate on locomotion activity in wild-type mice vs gene-targeted mice was examined. A rotarod test was performed using (*B*) caspase-1 / (F) or wild-type (E) mice, (*C*) IL-1RI / (F) or wild-type (E) mice, (*D*) MyD88 / (F) or wild-type (E) mice, (*G*) IL-18 / (F) or wild-type (E) mice, and (*H*) IL-18R / mice or wild-type (E) mice as mentioned above. *E* and *F*, Effect of kainate on locomotion activity in mice with different ages and genetic backgrounds was examined. A rotarod test was performed using either C57BL/6 mice (*E*) or BALB/c mice (*F*) 6- to 10-wk old. At time 0, kainate was injected. , p 0.05 when compared with the average data before kainate injection (n 5). #, p 0.05 when compared with wild-type mice (n 5). Data are represented as the mean SEM.

Intracerebellar injection

Mice were lightly anesthetized with ethyl alcohol (wake up time: 20 s). The solution (0.5 l) was injected into the center of the cerebellum using a 27G needle with a stopper held 2 mm from the top of the needle and a microsyringe pump system.

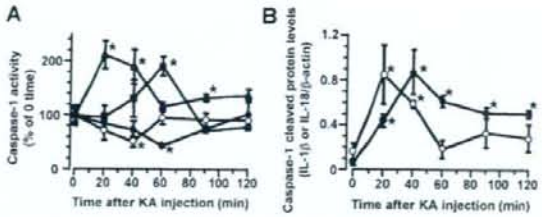

FIGURE 2. Systemic administration of kainate activates caspase-1, IL-1 , and IL-18 predominantly in cerebellum. Kainate (KA, 20 mg/kg) was i.p. injected into normal BALB/c mice and activity of caspase-1, IL-1 , and IL-18 was assessed. *A*, Activity of caspase-1 in cerebral cortex (E), cerebellum (,), hippocampus (f), and spinal cord ( ) was examined at various times after kainate-injection. Y-axis shows the percentage of caspase-1 activity compared with that at time 0. , p 0.05 when compared with the data at time 0 in each brain sample (n 4). *B*, Caspase-1-processed protein levels of IL-1 and IL-18 in cerebellum were analyzed after systemic administration of kainate. Extracts from various parts of brain were separated on SDS-PAGE, and activated IL-1 (E) and IL-18 (F) were detected with immunoblotting. Y-axis shows the relative protein levels of activated IL-1 and IL-18 that are normalized with the protein level of -actin (n 3). Because significant levels of activated IL-1 and IL-18 were not detected in the cerebral cortex, hippocampus, and spinal cord, their data are omitted. Data are represented as the mean SEM.

Behavioral experiment

To estimate the effect of kainate and the other reagents on behavioral activity, a rotarod test was performed. To this end, Rota-Rod Treadmill (Ugo Basile) that consists of a gritted plastic rod flanked by two large round plates was used. Before performing the test, mice were trained on the rotarod until they reached a stable performance in this test (120 s on rotarod) for one or two days before experiments. The test session was performed in accordance with the training session. Mice were brought to the experimental room at least 1 h before the experiment, and then placed on the accelerating rotarod apparatus (Ugo Basile Accelerating Rota-Rod "Jones & Roberts" for Rats 7750) with an initial speed of four rotations per

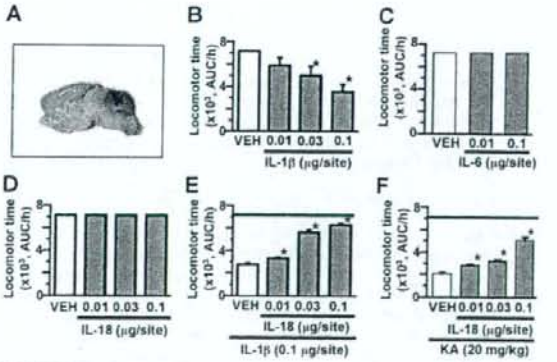

FIGURE 3. Intracerebellar injection of IL-1 induces ataxia, but intracerebellar injection of IL-18 together with IL-1 counteracted the effect of IL-1 in normal mice. *A*, Evans blue (0.5 l) was intracerebellarly injected and its distribution was examined. *B–F*, Effect of intracerebellar injection of IL-1 , IL-18, or IL-6 on locomotion activity was examined. Various doses of IL-1 (*B*), IL-6 (*C*), IL-18 (*D*), or IL-18 with IL-1 (0.1 nmol/site) (*E*) were intracerebellarly injected and rotarod test was performed as mentioned in Fig. 1. *F*, Five min after intracerebellar injection of various doses of IL-18, kainate (KA, 20 mg/kg) was i.p. administered, and a rotarod test was performed. Y-axis shows the area under the curve (AUC) for 1 h after injection. , p 0.05 when compared with vehicle (VEH: saline)-treated group (n 5). Dashed line shows the data from vehicle-treated group (*E*, without IL-1 ; *F*, without kainate). Data are represented as the mean SEM.

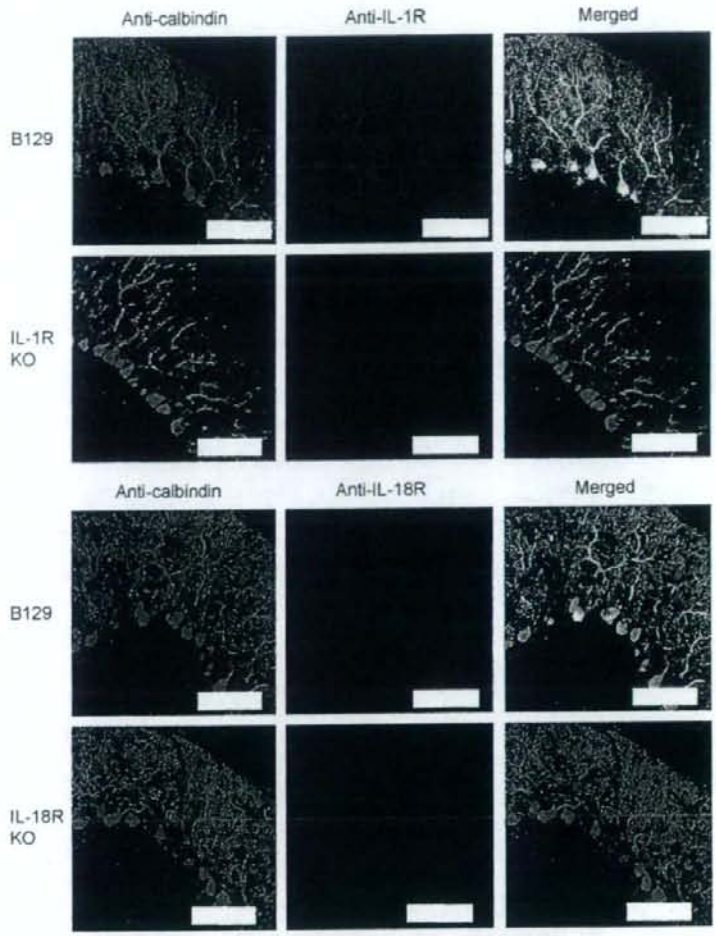

FIGURE 4. Immunohistochemical analysis of IL-1R and IL-18R in cerebellum is performed after the isolation of cerebellum from either normal mice, IL-1R / mice, or IL-18R / mice. The tissue section was stained with Ab to either IL-1RI or IL-18R, and then reacted with Alexa564-conjugated anti-rabbit or anti-goat IgG. To identify Purkinje cells, tissue sections were stained with Ab to calbindin, followed by Alexa488-conjugated anti-rabbit or anti-goat IgG. Fluorescent signals were detected using a confocal microscope. Scale bar, 100 m.

minute; thereafter, the speed gradually increased to 60 rotations per minute. The time that the mouse remained on the rod was measured. A maximum of 120 s was allowed to test each animal. In the rotarod test, mice were pretreated with reagents or the vehicle, and the experiment was started 20 min after treatment.

Caspase-1 activity

Cell lysates were prepared by homogenizing the tissues (cerebral cortex, cerebellum, hippocampus, or spinal cord) in lysis buffer, centrifuged at 10,000 *g* for 5 min at 4°C, and the supernatant was harvested. After determining the protein concentration, the cell lysates were used to measure the activity of caspase-1 using *N*-acetyl-Tyr-Val-Ala-Asp-*P*-nitroanilide as a substrate (Medical and Biological Laboratories). The reaction mixture was incubated for 2 h at 37°C. Caspase-1 activity was monitored with the absorbance at 420 nm, reacting chromophore *P*-nitroanilide.

Western blotting

Tissue samples (cerebral cortex, cerebellum, hippocampus, spinal cord) were homogenized in cell lysis buffer containing 137 mM NaCl, 20 mM Tris-HCl (pH 7.5), 1% Nonidet P-40, 10% glycerol, 1 mM PMSF, 10 g/ml aprotinin, and 1 g/ml leupeptin. The total protein concentration was determined using a Bio-Rad protein assay kit. Proteins were separated by electrophoresis using a 10 or 16% SDS-polyacrylamide gel and then transferred to a polyvinylidene fluoride membrane. The membrane was preincubated with a 5% skim milk solution for 1 h at room temperature, then incubated with primary Ab to either IL-1 or IL-18 at 4°C overnight, and subsequently incubated with a HRP-linked Ab against either mouse, rabbit, or goat IgG for 1 h. Membrane-bound HRP-labeled protein bands were reacted with a chemiluminescence detection solution (Amersham Biosciences). Chemiluminescent signals were detected using x-ray film. The amount of active IL-1 and IL-18 was evaluated by measuring the density of the active form cleaved by caspase-1 (17kD and 18 kD, respectively) using the National Institutes of Health Image program. The data were normalized with -actin.

Immunohistochemistry

Mice were anesthetized with ethyl carbamate (1.5g/kg, i.p.) and perfused with 4% paraformaldehyde following PBS (pH 7.4). The mouse cerebellum was then isolated. The tissue was soaked in 4% paraformaldehyde for 4 h and then in 30% sucrose solution overnight at 4°C. A section (30 m) was prepared using a cryostat. After washing with PBS, the section was soaked in PBS containing 0.3% Triton X-100 for 30 min and then in PBS containing 0.1% FBS for 30 min. The tissue section was incubated with the first Ab to either GluR-5, GluR-6, IL-1, IL-18, IL-1RI, IL-18R, calbindin, or glial fibrillary acidic protein overnight at 4°C, then washed with PBS, and reacted with Alexa488- or Alexa564-conjugated anti-IgG for 2 h. After washing with PBS, the sections were mounted with PBS/glycerol containing 0.05% triethylenediamine. Fluorescent signals were detected using a confocal microscope (Bio-Rad).

Data processing

All data are represented as the mean SEM. Statistical significance was analyzed using one-way ANOVA followed by Dunnett's multiple comparisons or Student's *t* test; p 0.05 was considered significant.

Results

Involvement of caspase-1 and IL-1 signaling in kainate-induced ataxia

The effect of kainate on motor coordination in mice was examined with the rotarod test (26), as judged by a decrease in latency before falling from a rotating rod. An i.p. injection of kainate (20 mg/kg), but not saline as a vehicle, induced ataxic gait (Fig. 1*A*). The retention time on the rotating rod was decreased at 20 min and the effect was almost abolished by 90 min after injection (Fig. 1*A*). Because IL-1 is indicated to play a critical role in seizures (16–20) and kainate is reported to increase in IL-1 transcripts in several regions of the brain (27), we considered whether kainate-induced ataxia might be mediated by IL-1 . To verify this possibility, we first examined the effect of kainate on caspase-1 / mice in which IL-1 cannot be activated. Interestingly enough, kainate showed almost no effect on motor coordination in caspase-1 / mice (Fig. 1*B*), suggesting that IL-1 is involved in kainate-induced ataxia. We then examined the effect of kainate injection in IL-1 receptor type I (IL-1RI) / mice. We found that kainate showed little effect, if any, on the motor coordination of IL-1RI / mice (Fig. 1*C*). Because MyD88 is reported to play a central role in IL-1 -mediated signal transduction (28), we then examined the effect of kainate in mice deficient in MyD88. We found that the effect of kainate was limited in MyD88 / mice as seen in IL-1RI / mice (Fig. 1*D*). Next, we examined whether the difference of ages and genetic backgrounds showed the different susceptibility to kainate-induced ataxia using various ages (six to 10 wk old) of C57BL/6 (Fig. 1*E*) or BALB/c mice (Fig. 1*F*), because we used caspase-1 / mice on a BALB/c background and IL-1RI / or MyD88 / mice on a C57BL/6 background of 6- to 10-wk-old. The result showed that the time courses of ataxia-induction and its recovery after systemic administration of kainate were corresponding in different ages of BALB/c or C57BL/6 mice. Taken together, these results indicate that i.p. injection of kainate induces ataxia gait in mice through the activation of caspase-1 and IL-1 .

Activation of caspase-1 and IL-1 in cerebellum with systemic administration of kainate

Next, we examined which region in the brain caspase-1 and IL-1 is activated. Caspase-1 activity was measured in various regions of the brain after kainate administration, and specifically increased in the cerebellum as well as hippocampus, but not in the cerebral cortex or spinal cord (Fig. 2*A*). Kinetic study showed that activity in the cerebellum peaked within 20 min and returned to the basal level by 60–90 min, while activity in the hippocampus peaked within 60 min and fell to the basal level by 90 min (Fig. 2*A*). Because ataxia was induced within 20 min after kainate administration, it is conceivable that kainate-induced activation of caspase-1 in the cerebellum evoked IL-1 activation and gait disturbance in mice. We then examined the expression of activated IL-1 at the protein level in various regions of the brain by Western blotting (Fig. 2*B*). As the precursor form of IL-1 is processed with caspase-1, their active form can be detected by the decrease of their m.w. IL-1 was activated within 20 min after kainate injection in the cerebellum (Fig. 2*B*), but was not detected in the cerebral cortex, hippocampus, or spinal cord (data not shown). Although it has been reported that kainate induced the increase in IL-1 mRNA in the cerebral cortex, thalamus, and hypothalamus (27), it remains unclear whether IL-1 is activated at the protein level in these loci. Our results show that systemic administration of kainate activates IL-1 predominantly in the cerebellum and indicates that this activation may play a critical role in kainate-induced ataxia.

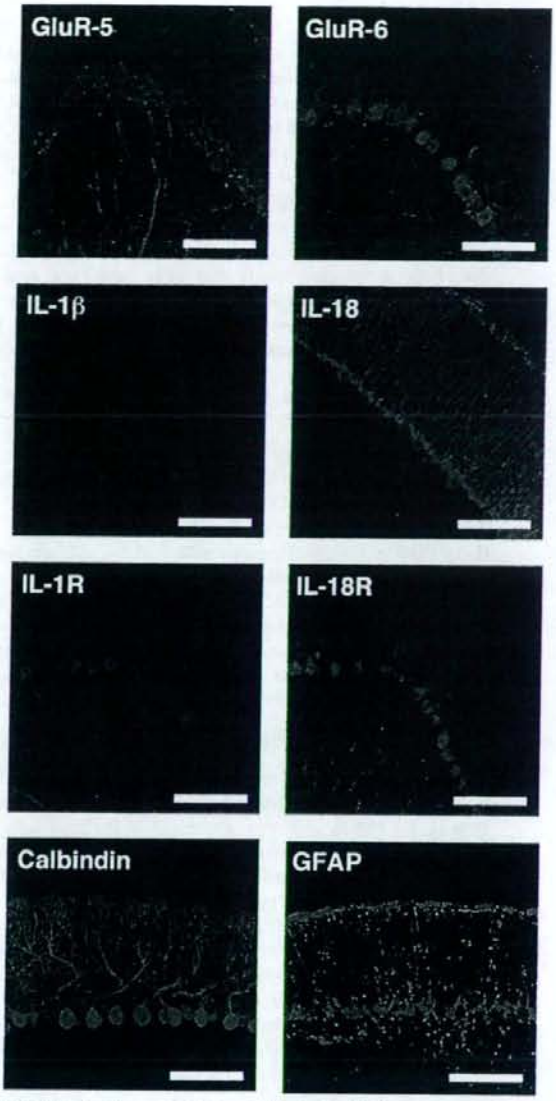

FIGURE 5. Immunohistochemical analysis of kainate receptors, IL-1, IL-18, IL-1R, and IL-18R in cerebellum was performed after isolation of cerebellum from normal mice. The tissue section was prepared and stained with Ab to either GluR5, GluR6, IL-1 , IL-18, IL-1RI, IL-18R , calbindin, or glial fibrillary acid protein (GFAP), then followed with FITC-conjugated anti-IgG for 1 h. Fluorescent signals were detected using a confocal microscope. Scale bar, 100 m.

Direct injection of IL-1 to cerebellum induces ataxia

To verify the above possibility, we directly injected recombinant IL-1 into the cerebellum and examined the motor coordination. To confirm whether the intracerebellar injection was accurate, Evans blue solution (0.5 1 of 1% solution) was injected. As shown in Fig. 3*A*, Evans blue solution was spread only in the field of the cerebellum. An intracerebellar injection of IL-1 (0.01–0.1 g/site) induced ataxia in a dose-dependent manner (Fig. 3*B*). As a negative control, we injected IL-6 (0.01 and 0.1 g/site) intracerebellarly and observed no induction of ataxia (Fig. 3*C*), which confirmed the IL-1 -specific ataxia induction.

IL-18 is involved in the recovery phase of kainate-induced ataxia

Because casapse-1 also activates IL-18 (29), we examined the activation of IL-18 in the cerebellum after kainate i.p. injection. Like IL-1 , IL-18 was also activated in the cerebellum (Fig. 2*B*). The level of activated IL-18 in the cerebellum peaked within 40 min and activated IL-18 was still observed until 2 h after kainate injection. We then tested whether kainate induces ataxia in IL-18 / or IL-18R / mice (Fig. 1, *G* and *H*). Systemic administration of kainate induced ataxia in these mice within 20 min, as seen in wild-type mice. To our surprise, recovery from the kainate-induced ataxia was significantly delayed in these mice. Ataxic gait was still observed after 2 h in IL-18 / mice, and after 4 h in IL-18R / mice. The results posed the possibility that IL-18 may enhance the recovery phase of kainate-induced ataxia.

Intracerebellar injection of IL-18 counteracts the effect of IL-1 and kainate

To assess the possibility described above, we examined the effect of intracerebellar injection of IL-18 with or without IL-1 . As shown in Fig. 3*D*, an intracerebellar injection of only IL-18 (0.01–0.1 g/site) did not induce ataxia. Interestingly enough, intracerebellar injection of IL-18 (0.01–0.1 g/site) together with IL-1 dose-dependently inhibited IL-1 (0.1 g/site)-induced ataxia (Fig. 3*E*). Furthermore, pretreatment with IL-18 (0.01–0.1 g/site, intracerebellarly, at 10 min) inhibited kainate-induced ataxia in a dose-dependent manner (Fig. 3*F*). These results strongly indicate that IL-18 in the cerebellum may play an important role in the recovery phase of kainate-induced ataxia in mice by counteracting with IL-1 .

Expression of IL-1R and IL-18R on Purkinje cells

Finally, we investigated which cells in the cerebellum express IL-1R and IL-18R by immunohistochemistry. Fig. 4 shows that both IL-1R and IL-18R were expressed in Purkinje cells. Their specific expression was confirmed by staining tissue sections of either IL-1RI / mice or IL-18R / mice. We also examined the expression of kainate receptors, IL-1 , and IL-18 in the cerebellum by immunohistochemistry (Fig. 5). GluR5 was expressed in astrocytes (glial fibrillary acid protein-positive) as well as Purkinje cells (calbindin-positive), while GluR6 was mainly expressed in Purkinje cells. IL-1 was expressed mainly in Purkinje cells and IL-18 was expressed in both Purkinje cells and astrocytes. We could not clearly detect the expression of IL-1 or IL-18 in other cells, including microglias or granular cells.

Discussion

Kainate receptors are reported to be expressed in various regions in the brain, including the cerebellum, in rodents (5), and it has been demonstrated that kainate induced the expression of IL-1 transcripts in various regions in the brain (27). In the present study, we showed the kainate-induced processing of IL-1 and IL-18 in the cerebellum, and demonstrated that IL-1 plays an important role in inducing kainate-triggered ataxia and that IL-18 has a positive regulatory role in recovery from kainate-induced ataxia.

This effect of kainate was really induced via a kainate receptor in the cerebellum since i.p. administration of 2-amino-5-hydroxy-5-methyl-4-isoxazolepropion acid/kainate-receptor antagonists, 6,7-dinitroquinoxaline-2,3-dione (0.3–3 mg/kg), and 6-cyano-7-nitroquinoxaline-2,3-dione (0.3–3 mg/kg), 30 min before systemic administration of kainate (20 mg/kg) injection specifically and dose-dependently inhibited kainate-induced ataxia (data not shown). Furthermore, intracerebellar injection of 6,7-dinitroquinoxaline-2,3-dione (0.25–0.75 g/site) dose-dependently inhibited kainate-induced ataxia. These results indicate that the ataxia was induced specifically via 2-amino-5-hydroxy-5-methyl-4-isoxazolepropion acid/kainate receptors.

Resistance to kainate-induced ataxia of caspase-1-, IL-1R-, and MyD88-deficient mice (Fig. 1) suggested an important role of IL-1 in kainate-induced ataxia. Time course of caspase-1-activation and the resultant IL-1 -processing in the cerebellum was corresponding to that of kainate-induced ataxia (Fig. 1 and 2), and direct intracerebellar injection of IL-1 elicited the ataxia (Fig. 3). These results indicate the involvement of IL-1 in the cerebellum in kainate-induced ataxia. Regarding the relationship between IL-1 in the cerebellum and ataxia, it was reported that two ataxic mutant mice, staggerer mice with retinoic acid receptor-related orphan receptor (nuclear hormone receptor superfamily) deficiency (30) and lurcher mice with 2-glutamate receptor deficiency (31) showed abnormal IL-1 expression in the cerebellum (32). In these mice, the neurodegenerative effect of IL-1 was attributed to the cerebellar ataxia. Concerning kainate, it was reported that kainate-induced ataxia was due to its neurodegenerative effect (2, 11). In this study, we examined apoptosis in the cerebellum at various times (30 min to 24 h) after kainate injection using TUNEL methods; however, we could not observe any apoptotic cells in the cerebellum (data not shown). The result indicates that although kainate affects various regions in the brain to induce neurodegenerative effects, the neurodegenerative effect may not be the direct cause in kainate-induced and IL-1 -mediated cerebellar ataxia in mice. The other possible effect of IL-1 on kainate-induced ataxia is its regulatory effect on neurotransmitter systems. IL-1 was reported to be involved in the regulation of inhibitory as well as excitatory neurotransmitter systems (33), while Purkinje cells were reported to express -amino-butyric acid, an inhibitory neurotransmitter (34). Of note, -amino-butyric acid was indicated to be involved in fast cerebellar oscillation associated with ataxia in a mouse model of Angelman syndrome (35). Taken together, it is assumed that IL-1 might induce the release of -amino-butyric acid from Purkinje cells and inhibits neuronal activity, including that of Purkinje cells. In this context, we are electrophysiologically examining the effect of kainate, IL-1 or IL-18, or both on Purkinje cells in the cerebellum.

Among the molecules that affect kainate-induced ataxia, caspase-1 deficiency showed the most complete abrogation of kainate-induced ataxia, while deficiency of either IL-1RI or MyD88 showed partial effect (Fig. 1). It is reported that more of the IL-1 cytokine family may be activated with caspase-1 (36). Recently, IL-1-like cytokine, IL-33, that was activated with caspase-1 and its receptor, ST2, was demonstrated to exert its effect on the induction of Th2-associated cytokines (37). With this regard, we detected the expression of IL-33 and ST2 in cerebellum by RT-PCR and immunohistochemical method (data not shown). Further investigation is necessary to clarify a role of ST2/IL-33 signaling including other caspase-1-activated IL-1-like cytokine signaling in kainate-induced ataxia in a future study.

Concerning MyD88-deficient mice, partial resistance to the effect of kainate suggests that signaling molecules other than MyD88 could be involved in kainate-induced caspase-1-dependent ataxia. In this respect, signaling of the IL-1R/TLR family is finely and sophisticatedly tuned with multiple signaling molecules (38). For example, Toll/IL-1R domain-containing adaptor inducing IFN- -related adaptor molecule was reported to be involved in the TLR 4-mediated MyD88-independent signaling pathway, although MyD88 is involved in TLR 4 signaling (39).

It was reported that human purinergic receptor ($P2X_7$) modulates IL-1 and IL-18 processing and their release in response to

ATP in caspase-1-independent fashion (40). To examine a possibility whether $P2X_7$ is involved in kainate-induced ataxia, we examined the effect of oxidized ATP, one of $P2X_7$ receptor antagonists (41), on kainate-induced ataxia. An intracerebellar injection of oxidized ATP did not inhibit the kainate-induced ataxia during at least 60 min after kainate-injection (data not shown). Therefore, the result suggested that the participation of $P2X_7$ is little on the induction of kainate-induced ataxia. In accordance with our results, Nicklas et al. (42) showed that kainate decreased the content (or release) of ATP in cerebellar slices.

The most interesting finding in this study is that IL-18, another caspase-1-activated proinflammatory cytokine (12), counteracted the effect of IL-1 in the induction of ataxia with kainate. IL-18- and IL-18R-deficient mice showed the delay of recovery from kainate-induced ataxia (Fig. 1), and intracerebellar injection of IL-18 together with IL-1 inhibited the IL-1 -induced ataxia (Fig. 3). We assume three possible explanations for these results: firstly, IL-18 may induce the expression of IL-1ra that inhibits the binding of IL-1 to its receptor; secondly, IL-1 and IL-18 may exert their effects on different cells in the neuronal network in the cerebellum; thirdly, IL-1 and IL-18 may exert their effects on the same target cells but induce counteracting signals. As for the first possibility, we examined the effect of intracerebellar injection of IL-18 on IL-1ra mRNA expression. IL-18 did not affect the expression of IL-1ra mRNA expression significantly during 60 min after intracerebellar injection, compared with intracerebellar injection of vehicle only (data not shown). Because intracerebellar injection of IL-18 showed a counteracting effect on kainate-induced or IL-1 -induced ataxia within 60 min (Fig. 3), the result suggests that IL-1ra is not involved in the anti-ataxia effect of IL-18 in cerebellum. Regarding the second possibility, immunohistochemical analysis showed that both IL-1RI and IL-18R were expressed on Purkinje cells in the cerebellum (Fig. 4). The analysis indicated the expression of IL-18R but not IL-1RI on astrocytes (Fig. 5). Thus, IL-18 may counteract IL-1 by exerting its effect through different target cells. Concerning the third possibility, it has been so far reported that receptors for IL-1 and IL-18 use the same signaling module, MyD88 and IL-1-receptor associated kinases (43). However, because the receptors for both cytokines are expressed on Purkinje cells, it is possible that the receptors for these cytokines use a different signaling pathway in Purkinje cells. With this possibility, ST2, one of the IL-1 receptor family, has been described as a negative regulator for TLR-IL-1R signaling (44), in line with an earlier report that ST2 was unable to activate the IL-1-activated transcription factor NF- B (45, 46). The detailed mechanisms on the interaction of IL-1 and IL-18 in the induction and recovery of ataxia remain unknown. The electrophysiological examination might reveal the effect of kainate, IL-1 or IL-18, or both on neural network in the cerebellum.

Concerning the genetic background of knockout mice, we had used knockout mice of the same genetic backgrounds, i.e., C57BL/6 background for IL-1RI $^{-/-}$, MyD88 $^{-/-}$, IL-18 $^{-/-}$, and IL-18R $^{-/-}$ mice, but used a BALB/c background for caspase-1 $^{-/-}$ mice. Regarding the differences in the development of inflammatory disease of the IL-1ra $^{-/-}$ mice, Horai et al. (47) showed that the IL-1ra-deficient mice on a BALB/c background, but not those on a C57BL/6J background, spontaneously developed chronic inflammatory polyarthropathy. Their results suggested that genes other than IL-1ra are involved in the development of spontaneously developed arthritis. They also observed that IL-1ra $^{-/-}$ mice on the C57BL/6 background developed arthritis at a high incidence when these mice were immunized with type II collagen. Their result demonstrated that IL-1ra $^{-/-}$ mice on C57BL/6 background as well as BALB/c background showed the corresponding susceptibility to experimentally induced arthritis. In our study, we observed the effect of kainate on the acutely induced ataxia (induction within 20 min after the kainate injection and the following subsidence within 60–120 min). Our data showed that the mice deficient with IL-1RI, or MyD88 on the same C57BL/6 background were resistant to kainate-induced ataxia, while IL-18- or IL-18R -deficient mice on the same C57BL/6 background displayed significant delay of the recovery from ataxia. In these experiments, we had compared the responses with the wild-type mice on the same C57BL/6 background. We have also compared the locomotion time of normal BALB/c mice and C57BL/6 mice after systemic administration of kainate, and observed the similar responses in normal BALB/c mice and C57BL/6 mice (Fig. 1, *E* and *F*). Our data suggest that the effect of the genetic background of BALB/c mice and C57BL/6 mice on kainate-induced ataxia in the acute phase is less important. Taken together, our data clearly showed that IL-1RI or MyD88 was involved in the induction of ataxia, and IL-18 and its receptor in the recovery of the kainate-induced ataxia in the C57BL/6 genetic background.

Recently Zhang et al. (48) showed that IL-18-deficient mice were more sensitive to kainate administration in the induction of neurodegeneration compared with the normal animals. The observation that IL-18 deficiency aggravated kainate-induced hippocampal neurodegeneration seems similar to our observation that the mice with IL-18 deficiency showed a delay of the recovery from kainate-induced ataxia. However, they showed that the exogenous administration of IL-18 aggravated the kainate-induced neurodegeneration. They concluded that IL-18 had a disease-promoting role in kainate-induced excitotoxicity but that the roles of IL-18 in excitotoxic injury in IL-18-deficient mice might be overcompensated by an increase of other microglia-derived disease-promoting factors, such as IL-12. In contrast, we demonstrated that the exogenous administration of IL-18 showed the counteracting effect on kainate-induced ataxia (Fig. 3*F*). Our results suggest that although IL-18 and IL-1 are both proinflammatory cytokines, IL-18 showed the counteracting effect in kainate-induced ataxia.

In this study, we provided evidence that caspase-1 and IL-1RI in the cerebellum are essential for kainate-induced ataxia and that IL-18 and IL-18R are positive regulators for the recovery phase of kainate-induced ataxia in mice. Earlier reports on the effect of kainate have demonstrated its effect mainly in the hippocampus, and kainate is reported to show a neurodegenerative effect (2, 49). In this regard, the present study showed that caspase-1 was activated not only in the cerebellum but also in the hippocampus (Fig. 2). The activation of caspase-1 in the hippocampus peaked at 60 min after kainate administration, although ataxia was induced within 20 min and then gradually subsided within 60 to 90 min after kainate stimulation. In our studies, we could not detect either activated IL-1 or activated IL-18 at the protein level in the hippocampus, while we could clearly detect them in the cerebellum. Our result indicates that the activation of caspase-1 in the hippocampus may not be directly attributed to kainate-induced ataxia, but may lead to a neurodegenerative effect of kainate. Further analysis of the molecular as well as physiological basis of IL-1 -induced ataxia and its inhibition by IL-18 in the cerebellum may contribute to clarify the mechanism of kainate-induced ataxia, and might contribute toward the development of a new strategy for the therapy of cerebellar ataxia in humans.

Acknowledgments

We thank K. Kuida, K. Hoshino, and S. Akira for providing us with caspase-1 $^{-/-}$, IL-18R $^{-/-}$, and MyD88 $^{-/-}$ mice, respectively. We are also grateful to S. Hirota for taking care of the knock out mice.

Disclosures

The authors have no financial conflict of interest.

References

1. Ben-Ari, Y., and R. Cossart. 2000. Kainate, a double agent that generates seizures: two decades of progress. *Trends Neurosci.* 23: 580–587.
2. Mulle, C., A. Sailer, I. Pérez-Otaño, H. Dickinson-Anson, P. E. Castillo, I. Bureau, C. Maron, F. H. Gage, J. R. Mann, B. Bettler, and S. F. Hainemann. 1998. Altered synaptic physiology and reduced susceptibility to kainate-induced seizures in GluR6-deficient mice. *Nature* 392: 601–605.
3. Bettler, B., and C. Mulle. 1995. Review: neurotransmitter receptors: II. AMPA and kainate receptors. *Neuropharmacology* 34: 123–139.
4. Lerma, J., M. Morales, M. A. Vicente, and O. Herreras. 1997. Glutamate receptors of the kainate type and synaptic transmission. *Trends Neurosci.* 20: 9–12.
5. Bahn, S., B. Volk, and W. Wisden. 1994. Kainate receptor gene expression in the developing rat brain. *J. Neurosci.* 14: 5525–5547.
6. Bettler, B., J. Boulter, I. Hermans-Borgmeyer, A. O'Shea-Greenfield, E. S. Deneris, C. Moll, U. Borgmeyer, M. Hollmann, and S. Heinemann. 1990. Cloning of a novel glutamate receptor subunit, GluR5: expression in the nervous system during development. *Neuron* 5: 583–595.
7. Egebjerg, J., B. Bettler, I. Hermans-Borgmeyer, and S. Heinemann. 1991. Cloning of a cDNA for a glutamate receptor subunit activated by kainate but not AMPA. *Nature* 351: 745–748.
8. Feldmeyer, D., and S. Cull-Candy. Neurotransmitters: elusive glutamate receptors. 1994. *Curr. Biol.* 4: 82–84.
9. Herb, A., N. Burnashev, P. Werner, B. Sakmann, W. Sisden, and P. H. Seeburg. 1992. The KA-2 subunit of excitatory amino acid receptors shows widespread expression in brain and forms ion channels with distantly related subunits. *Neuron* 8: 775–785.
10. Werner, P., M. Voigt, K. Keinanen, W. Wisden, and P. H. Seeburg. 1991. Cloning of a putative high-affinity kainate receptor expressed predominantly in hippocampal CA3 cells. *Nature* 351: 742–744.
11. Meldrum, B., and J. Garthwaite. 1990. Excitatory amino acid neurotoxicity and neurodegenerative disease. *Trends Pharmacol. Sci.* 11: 379–387.
12. Dinarello, C. A. 1998. Interleukin-1 , interleukin-18, and the interleukin-1 converting enzyme. *Ann. NY Acad. Sci.* 856: 1–11.
13. Jander, S., M. Schroeter, and G. Stoll. 2002. Interleukin-18 expression after focal ischemia of the rat brain: association with the late-stage inflammatory response. *J. Cereb. Blood Flow Metab.* 22: 62–70.
14. Neveu, P. J., and S. Liége. 2000. Mechanisms of behavioral and neuroendocrine effects of interleukin-1 in mice. *Ann. NY Acad. Sci.* 917: 175–185.
15. Patel, H. C., H. Boutin, and S. M. Allan. 2003. Interleukin-1 in the brain: mechanisms of action in acute neurodegeneration. *Ann. NY Acad. Sci.* 992: 39–47.
16. Minami, M., Y. Kuraishi, T. Yamaguchi, S. Nakai, Y. Hirai, and M. Satoh. 1990. Convulsants induce interleukin-1 messenger RNA in rat brain. *Biochem. Biophys. Res. Commun.* 171: 832–837.
17. Nishiyori, A., M. Minami, S. Takami, and M. Satoh. 1997. Type 2 interleukin-1 receptor mRNA is induced by kainic acid in the rat brain. *Brain Res. Mol. Brain Res.* 50: 237–245.
18. Eriksson, C., R. Tehranian, K. Iverfeldt, B. Winblad, and M. Schultzberg. 2000. Increased expression of mRNA encoding interleukin-1 and caspase-1, and the secreted isoform of interleukin-1 receptor antagonist in the rat brain following systemic kainic acid administration. *J. Neurosci. Res.* 60: 266–279.
19. Vezzani, A., M. Conti, A. De Luigi, T. Ravizza, D. Moneta, F. Marchesi, and M. G. De Simoni. 1999. Interleukin-1 immunoreactivity and microglia are enhanced in the rat hippocampus by focal kainate application: functional evidence for enhancement of electrographic seizures. *J. Neurosci.* 19: 5054–5065.
20. Vezzani, A., D. Moneta, M. Conti, C. Richichi, T. Ravizza, A. De Luigi, M. G. De Simoni, G. Sperk, S. Andell-Jonsson, J. Lundkvist, et al. 2000. Powerful anticonvulsant action of IL-1 receptor antagonist on intracerebral injection and astrocytic overexpression in mice. *Proc. Natl. Acad. Sci. USA* 97: 11534–11539.
21. Felderhoff-Mueser, U., O. I. Schmidt, A. Oberholzer, C. Buhrer, and P. F. Stahel. 2005. IL-18: a key player in neuroinflammation and neurodegeneration? *Trends Neurosci.* 28: 487–493.
22. Duenas, A. M., R. Goold, and P. Giunti. 2006. Molecular pathogenesis of spinocerebellar ataxias. *Brain* 129: 1357–1370.
23. Taylor, A. M., and P. J. Byrd. 2005. Molecular pathology of ataxia telangiectasia. *J. Clin. Pathol.* 58: 1009–1015.
24. Kuida, K., J. A. Lippke, G. Ku, M. W. Harding, D. J. Livingston, M. S. Su, and R. A. Flavell. 1995. Altered cytokine export and apoptosis in mice deficient in interleukin-1 converting enzyme. *Science* 267: 2000–2003.
25. Hoshino, K., H. Tsutsui, T. Kawai, K. Takeda, K. Nakanishi, Y. Takeda, and S. Akira. 1999. Cutting edge: generation of IL-18 receptor-deficient mice: evidence for IL-1 receptor-related protein as an essential IL-18 binding receptor. *J. Immunol.* 162: 5041–5044.
26. Pietraszek, M., A. Gravius, D. Schafer, T. Weil, D. Trifanova, and W. Danysz. 2005. mGluR5, but not mGluR1, antagonist modifies MK-801-induced locomotor activity and deficit of prepulse inhibition. *Neuropharmacology* 49: 73–85.
27. Minami, M., Y. Kuraishi, and M. Satoh. 1991. Effects of kainic acid on messenger RNA levels of IL-1 , IL-6, TNF , and LIF in the rat brain. *Biochem. Biophys. Res. Commun.* 176: 593–598.
28. Adachi, O., T. Kawai, K. Takeda, M. Matsumoto, H. Tsutsui, M. Sakagami, K. Nakanishi, and S. Akira. 1998. Targeted disruption of the MyD88 gene results in loss of IL-1- and IL-18-mediated function. *Immunity* 9: 143–150.
29. Gu, Y., K. Kuida, H. Tsutsui, G. Ku, K. Hsiao, M. A. Fleming, N. Hayashi, K. Higashino, H. Okamura, K. Nakanishi, et al. 1997. Activation of interferon-inducing factor mediated by interleukin-1 converting enzyme. *Science* 275: 206–209.
30. Hamilton, B. A., W. N. Frankel, A. W. Kerrebrock, T. L. Hawkins, W. FitzHugh, K. Kusumi, L. B. Russell, K. L. Mueller, V. van Berkel, B. W. Birren, et al. 1996. Disruption of the nuclear hormone receptor ROR in staggerer mice. *Nature* 379: 736–739.
31. Zuo, J., P. L. De Jager, K. A. Takahashi, W. Jiang, D. J. Linden, and N. Heintz. 1997. Neurodegeneration in Lurcher mice caused by mutation in 2 glutamate receptor gene. *Nature* 388: 769–773.
32. Vernet-der Garabedian, B., Y. Lemaigre-Dubreuil, N. Delhaye-Bouchaud, and J. Mariani. 1998. Abnormal IL-1 cytokine expression in the cerebellum of the ataxic mutant mice staggerer and lurcher. *Brain Res. Mol. Brain Res.* 62: 224–227.
33. Miller, L. G., and J. M. Fahey. 1994. Interleukin-1 modulates GABAergic and glutamatergic function in brain. *Ann. NY Acad. Sci.* 739: 292–298.
34. Gabbott, P. L., J. Somogyi, M. G. Stewart, and J. Hamori. 1986. GABA-immunoreactive neurons in the rat cerebellum: a light and electron microscope study. *J. Comp. Neurol.* 251: 474–490.
35. Cheron, G., L. Servais, J. Wagstaff, and B. Dan. 2005. Fast cerebellar oscillation associated with ataxia in a mouse model of Angelman syndrome. *Neuroscience* 130: 631–637.
36. Sims, J. E., M. J. Nicklin, J. F. Bazan, J. L. Barton, S. J. Busfield, J. E. Ford, R. A. Kastelein, S. Kumar, H. Lin, J. J. Mulero, et al. 2001. A new nomenclature for IL-1-family genes. *Trends Immunol.* 22: 536–537.
37. Schmitz, J., A. Owyang, E. Oldham, Y. Song, E. Murphy, T. K. McClanahan, G. Zurawski, M. Moshrefi, J. Qin, X. Li, et al. 2005. IL-33, an interleukin-1-like cytokine that signals via the IL-1 receptor-related protein ST2 and induces T helper type 2-associated cytokines. *Immunity* 23: 479–490.
38. Takeda, K., and S. Akira. 2005. Toll-like receptors in innate immunity. *Int. Immunol.* 17: 1–14.
39. Yamamoto, M., S. Sato, H. Hemmi, S. Uematsu, K. Hoshino, T. Kaisho, O. Takeuchi, K. Takeda, and S. Akira. 2003. TRAM is specifically involved in the Toll-like receptor 4-mediated MyD88-independent signaling pathway. *Nat. Immunol.* 4: 1144–1150.
40. Mehta, V. B., J. Hart, and M. D. Wewers. 2001. ATP-stimulated release of interleukin (IL)-1 and IL-18 requires priming by lipopolysaccharide and is independent of caspase-1 cleavage. *J. Biol. Chem.* 276: 3820–3826.
41. Murgia, M., S. Hanau, P. Pizzo, M. Rippa, and F. Di Virgilio. 1993. Oxidized ATP: an irreversible inhibitor of the macrophage purinergic P2Z receptor. *J. Biol. Chem.* 268: 8199–8203.
42. Nicklas, W. J., B. Krespan, and S. Berl. 1980. Effect of kainate on ATP levels and glutamate metabolism in cerebellar slices. *Eur. J. Pharmacol.* 62: 209–213.
43. Bowie, A., and L. A. O'Neill. 2000. The interleukin-1 receptor/Toll-like receptor superfamily: signal generators for pro-inflammatory interleukins and microbial products. *J. Leukocyte Biol.* 67: 508–514.
44. Brint, E. K., D. Xu, H. Liu, A. Dunne, A. N. McKenzie, L. A. O'Neill, and F. Y. Liew. 2004. ST2 is an inhibitor of interleukin 1 receptor and Toll-like receptor 4 signaling and maintains endotoxin tolerance. *Nat. Immunol.* 5: 373–379.
45. Thomassen, E., B. R. Renshaw, and J. E. Sims. 1999. Identification and characterization of SIGIRR, a molecule representing a novel subtype of the IL-1R superfamily. *Cytokine* 11: 389–399.
46. Brint, E. K., K. A. Fitzgerald, P. Smith, A. J. Coyle, J. C. Gutierrez-Ramos, P. G. Fallon, and L. A. O'Neill. 2002. Characterization of signaling pathways activated by the interleukin 1 (IL-1) receptor homologue T1/ST2: a role for Jun N-terminal kinase in IL-4 induction. *J. Biol. Chem.* 277: 49205–49211.
47. Horai, R., S. Saijo, H. Tanioka, S. Nakae, K. Sudo, A. Okahara, T. Ikuse, M. Asano, and Y. Iwakura. 2000. Development of chronic inflammatory arthropathy resembling rheumatoid arthritis in interleukin 1 receptor antagonist-deficient mice. *J. Exp. Med.* 191: 313–320.
48. Zhang, X. M., R. S. Duan, Z. Chen, H. C. Quezada, E. Mix, B. Winblad, and J. Zhu. 2007. IL-18 deficiency aggravates kainic acid-induced hippocampal neurodegeneration in C57BL/6 mice due to an overcompensation by IL-12. *Exp. Neurol.* 205: 64–73.
49. Yang, D. D., C. Y. Kuan, A. J. Whitmarsh, M. Rincon, T. S. Zheng, R. J. Davis, P. Rakic, and R. A. Flavell. 1997. Absence of excitotoxicity-induced apoptosis in the hippocampus of mice lacking the Jnk3 gene. *Nature* 389: 865–870.

nature medicine

Interferon-g is a therapeutic target molecule for prevention of postoperative adhesion formation

Hisashi Kosaka[1,5], Tomohiro Yoshimoto[2,3,5], Takayuki Yoshimoto[4], Jiro Fujimoto[1] & Kenji Nakanishi[2,3]

Intestinal adhesions are bands of fibrous tissue that connect the loops of the intestine to each other, to other abdominal organs or to the abdominal wall[1–3]. Fibrous tissue formation is regulated by the balance between plasminogen activator inhibitor type 1 (PAI-1) and tissue-type plasminogen activator (tPA), which reciprocally regulate fibrin deposition. Several components of the inflammatory system, including cytokines[4], chemokines, cell adhesion molecules and neuropeptide substance P, have been reported to participate in adhesion formation[4–7]. We have used cecal cauterization to develop a unique experimental mouse model of intestinal adhesion. Mice developed severe intestinal adhesion after this treatment. Adhesion development depended upon the interferon-c (IFN-c) and signal transducer and activator of transcription-1 (STAT1) system. Natural killer T (NKT) cell–deficient mice developed adhesion poorly, whereas they developed severe adhesion after reconstitution with NKT cells from wild-type mice, suggesting that NKT cell IFN-c production is indispensable for adhesion formation. This response does not depend on STAT4, STAT6, interleukin-12 (IL-12), IL-18, tumor necrosis factor-a, Toll-like receptor 4 or myeloid differentiation factor-88–mediated signals. Wild-type mice increased the ratio of PAI-1 to tPA after cecal cauterization, whereas $Ifng^{-/-}$ or $Stat1^{-/-}$ mice did not, suggesting that IFN-c has a crucial role in the differential regulation of PAI-1 and tPA. Additionally, hepatocyte growth factor, a potent mitogenic factor for hepatocytes[8,9], strongly inhibited intestinal adhesion by diminishing IFN-c production, providing a potential new way to prevent postoperative adhesions.

Abdominal adhesion formation occurs in 67–93% of abdominal surgeries[10–13]. Adhesion also develops after abdominal bacterial infections, such as peritonitis[14]. A recent study has indicated that T helper type 1 (T_H1) cells are essential for the development of adhesion in a mouse model of intra-abdominal sepsis[15]. Nevertheless, only a limited number of studies have investigated the molecular process involved in intestinal adhesions. In addition, there are no appropriate treatments for or ways to prevent intestinal adhesions. Here we have established a unique experimental mouse model for elucidating the molecular mechanism underlying organ adhesions.

We induced intestinal adhesion by cecal cauterization using the coagulation mode of bipolar forceps. A time-course experiment revealed that this treatment induced progressive inflammatory and fibrotic changes (Supplementary Fig. 1a online). Adhesions strongly connected the cecum to the large bowel, the abdominal wall or both at day 7. Wild-type mice formed thick adhesion with plantar attachment (which we gave a score of 4) or developed very thick vascularized adhesion (score 5; Supplementary Fig. 1b). This fibrotic structure was firm and difficult to remove from the involved organs. In contrast, mice that underwent control laparotomy without cecal cauterization had no adhesion (score 0; Supplementary Fig. 1b).

To understand the immunological mechanism underlying cauterization-induced intestinal adhesion, we examined mice depleted of $CD4^+$T cells for their capacity to develop adhesion (Fig. 1). These mice had significantly reduced adhesion (score 0 or 1) and fibrotic changes in their ceca, compared with control mice (score 5) ($P < 0.0001$; Fig. 1a,c), suggesting that $CD4^+$T cells are essential in adhesion formation.

Because $CD4^+$ T cells consist of conventional $NK1.1^-CD4^+$ T cells and NKT cells expressing ab T cell receptor with invariant Va14–Ja18 (refs. 16–18), we examined which type of $CD4^+$ T cells contributed to this adhesion formation. Thus, we surgically treated NKT cell–deficient mice[19] by cauterizing isolated ceca and examined their intestinal adhesion formation. These mice developed lower grade (score 1 or 2; $P < 0.0001$) intestinal adhesion and weak fibrotic change (Fig. 1b,c). However, when they were reconstituted with unfractionated $CD4^+$ T cells from wild-type mice, but not from $Ifng^{-/-}$ mice, they gained the capacity to develop severe intestinal adhesion and severe fibrotic changes (Fig. 1b,c). Thus, unlike in a previous mouse model of surgical adhesion formation in which T_H1 cells were essential[15], in our adhesion model NKT cells contributed to intestinal adhesion formation by producing IFN-g.

In general, cytokine messenger RNAs, including IFN-g mRNA, are undetectable in the cecum. However, surgical treatment induced cecum IFN-g mRNA expression, which peaked at 3 h and declined gradually, suggesting immediate IFN-g production by NKT cells

[1]Department of Surgery and [2]Department of Immunology and Medical Zoology, Hyogo College of Medicine, 1-1, Mukogawa, Nishinomiya, Hyogo 663-8501, Japan. [3]Core Research for Evolutional Science and Technology, Japan Science and Technology Corporation, 4-1-8, Honmachi, Kawaguchi, Saitama 332-0012, Japan. [4]Intractable Immune System Disease Research Center, Tokyo Medical University, 6-1-1, Shinjuku, Shinjuku-ku, Tokyo 160-8402, Japan. [5]These authors contributed equally to this work. Correspondence should be addressed to K.N. (nakaken@hyo-med.ac.jp).

Received 13 September 2007; accepted 4 February 2008; published online 16 March 2008; doi:10.1038/nm1733

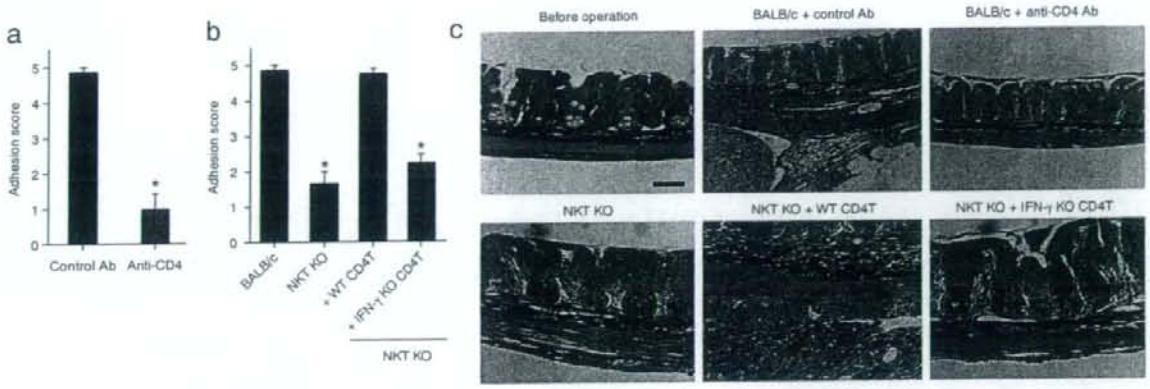

Figure 1 NKT cells are the main contributors to postsurgical adhesion formation. (a,b) BALB/c mice or BALB/c mice depleted of CD4+ T cells by treatment with antibody to CD4, anti-CD4 (a) or NKT cell-deficient (NKT KO) mice or NKT KO mice reconstituted with splenic CD4+ T cells (1.0 10^7 cells per mouse) from wild-type (WT CD4T) or Ifng$^{-/-}$ (IFN-g KO) mice (b) as described in the Methods underwent cecal cauterization surgery. Seven days after operation, mice were killed and examined for adhesion formation. Results are geometric means ± s.e.m. of eight mice per group and are representative of more than three independent experiments. *P o 0.0001 as compared to BALB/c control groups. (c) Seven days after cecal cauterization surgery, each group of mice (as described in a and b) were killed and the isolated ceca were stained with Sirius red. Representative results from eight to ten mice per group are shown. Scale bar, 50 mm.

(Fig. 2a). NKT cell–deficient mice had lower expression of IFN-g mRNA in their ceca (Fig. 2b), further substantiating this possibility. We next examined the capacity of Ifng$^{-/-}$ mice or Stat1$^{-/-}$ mice, which lack molecules required for intracellular signaling of IFN-g, IFN-a and IFN-b (ref. 20), to develop abdominal adhesion (Fig. 2c,d). Both types of mice did not develop abdominal adhesion. However, only Ifng$^{-/-}$ mice gained the capacity to develop intestinal adhesion after administration of IFN-g (Fig. 2c). Next, we examined whether surgical adhesion formation rapidly induced accumulation of NKT cells in the cecal wall. We found a marked and rapid increase in the number of

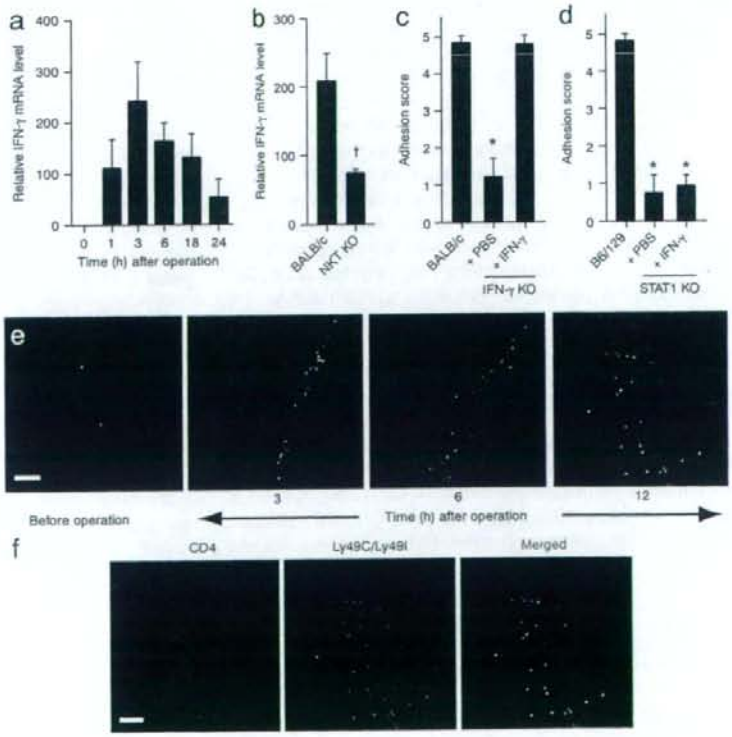

Figure 2 Rapid IFN-g production by NKT cells is causative in postsurgical adhesion formation. (a) Relative IFN-g mRNA expression in isolated cecum from BALB/c mice that had undergone cecal cauterization surgery as determined by real-time PCR. Cecum was isolated before and 1, 3, 6, 18 and 24 h after operation. (b) Relative IFN-g mRNA expression in isolated cecum from BALB/c and NKT KO mice 3 h after cecal cauterization surgery as determined by real-time PCR. Results are geometric means ± s.e.m. of five to eight mice per group and are representative of two independent experiments. wP o 0.05 as compared to control wild-type mice. (c,d) BALB/c mice, IFN-g KO mice (c) and Stat1$^{-/-}$ mice (STAT1 KO; d) injected with PBS or IFN-g by osmotic pumps as described in the Methods underwent cecal cauterization surgery. Seven days after operation, mice were killed and examined for adhesion formation. Results are geometric means ± s.e.m. of five mice per group and are representative of three independent experiments. *P o 0.0001 as compared to control wild-type mice. (e,f) After cecal cauterization, mice were killed and their ceca were taken and frozen at the indicated times (e) and at 12h (f). Frozen sections were fixed and incubated with antibodies to mouse Ly49C/Ly49I and CD4 and then examined by confocal microscopy. CD4, red; Ly49C/Ly49I, green; colocalization, yellow (Merged). Scale bar, 50 mm.

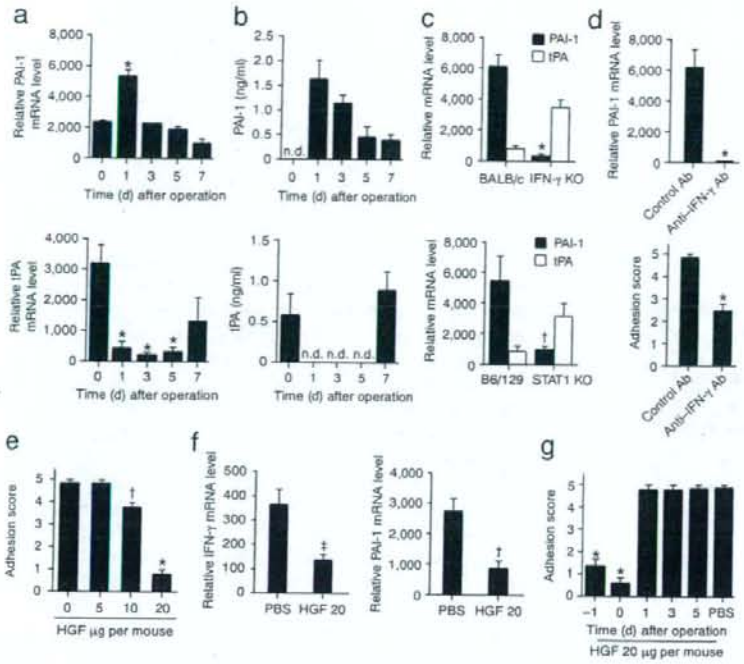

Figure 3 HGF inhibits IFN-g–STAT1–dependent PAI-1 induction and postsurgical adhesion formation. (a–g) BALB/c mice underwent cecal cauterization surgery. The relative mRNA expression of PAI-1 (a,c,d,f) and tPA (a,c) in isolated cecum, PAI-1 and tPA levels in the plasma (b), and adhesion score (d,e,g) were measured (see Methods). (a,b) Ceca and plasma were taken at the indicated days after operation. (c) Ceca were taken 1 d after operation. Results are geometric means ± s.e.m. of five mice per group and are representative of three independent experiments. *P o 0.005 as compared to non-operated control group (a). n.d., not detected (b). *P o 0.0001 and wP o 0.02 as compared to control mice group, respectively (c). (d) Ceca (top) were taken from BALB/c mice injected with IFN-g–specific or control antibodies 2 d before and subsequently treated with cecal cauterization 1 d before. Adhesion formation (bottom) at 7 d after operation was examined. Results are representative of two independent experiments. *P o 0.002 as compared to control groups. (e–g) BALB/c mice were injected with HGF (0–20 mg per mouse) 1 d before cecal cauterization (e,f) or on the days indicated (g). Adhesion formation (bottom) was examined at 7 d after operation (e,g). Three hours and 1 d after operation, the relative IFN-g and PAI-1 mRNA expression in isolated cecum was determined (f). Representative of three independent experiments. *P o 0.0001, wP o 0.005 and zP o 0.02 as compared to control PBS-injected mice.

Ly49$^+$CD4$^+$ T cells (NKT cells)[21] at 3 h after operation (Fig. 2e,f), further substantiating the idea that NKT cells are responsible for rapid IFN-g production after surgical treatment.

Postsurgical adhesion formation in an intra-abdominal septic model was reported to be dependent on the action of CD4$^+$ T_H1 cells[15]. Therefore, we examined whether the T_H1 response or the lipopolysaccharide (LPS) or tumor necrosis factor-a (TNF-a) responses can affect the development of cauterization-induced intestinal adhesion. We have summarized the results in Supplementary Table 1 online. *Stat4*$^{-/-}$ (ref. 22), *Stat6*$^{-/-}$ (ref. 23), *Il12p40*$^{-/-}$ and *Il18*$^{-/-}$ mice normally developed postsurgical abdominal adhesion. Furthermore, C3H/HeJ mice, which have a point mutation in the gene encoding Toll-like receptor 4 (TLR4), *Myd88*$^{-/-}$ mice, which lack an adaptor protein for TLRs, and *Tnfa*$^{-/-}$ mice also normally developed abdominal adhesion (Supplementary Table 1). Therefore, our adhesion model is non–LPS-induced, and T_H1 cells, T_H2 cells, TNF-a or TLR-MyD88–induced signals are not involved. Additionally, this surgical treatment induced the expression of mRNAs for IL-1b, IL-6, IL-17, TNF-a and TGF-b (Supplementary Fig. 2 online).

The proinflammatory neuropeptide substance P can initiate a wide range of adhesiogenic effects[24]. Therefore, *Tac1*$^{-/-}$ mice, lacking tachykinins, including substance P, neurokinin A, neuropeptide K and neuropeptide g (ref. 25), were tested in their capacity to develop intestinal adhesion. They had a significantly reduced adhesion score (P o 0.001; Supplementary Fig. 3a online) and reduced IFN-g mRNA expression in their ceca (Supplementary Fig. 3b). Furthermore, CD4$^+$ T cells from wild-type mice, but not from NKT cell–deficient mice, produced IFN-g in response to substance P and increased further IFN-g production when additionally stimulated with neurokinin A and neuropeptide K (Supplementary Fig. 3c). These results strongly suggest that tachykinins induce NKT cell IFN-g production.

Because fibrinolysis is regulated by PAI-1 and tPA activity[1,26], we examined whether the ratio of these molecules is regulated by surgical treatment via IFN-g–dependent STAT1 activation. Wild-type mice had increased expression of PAI-1 and decreased expression of tPA, both in their ceca (at the mRNA level) and in their plasma (at the protein level) at day 1 (Fig. 3a,b), whereas *Ifng*$^{-/-}$ or *Stat1*$^{-/-}$ mice did not (Fig. 3c), suggesting reciprocal regulation of PAI-1 and tPA activity by IFN-g. Furthermore, wild-type mice pretreated with a single injection of IFN-g–specific antibody (2 mg per mouse) one day before cecal cauterization did not show an increase in PAI-1 mRNA and had significantly less intestinal adhesion (score 2) (P o 0.002; Fig. 3d). Thus, IFN-g is a causative factor in postsurgical adhesion formation.

We have previously reported that hepatocyte growth factor (HGF) treatment strongly suppresses IFN-g mRNA expression in the small intestines of mice with acute graft-versus-host disease[27]. Thus, we injected recombinant HGF protein (5, 10 or 20 mg per mouse) subcutaneously 1 d before operation to examine its preventive effects on adhesion formation. A single injection of HGF (20 mg per mouse) significantly reduced intestinal adhesion (score 0 or 1; Fig. 3e). Furthermore, HGF treatment suppressed mRNAs for IFN-g and PAI-1, suggesting that HGF inhibits PAI-1 via inhibition of IFN-g production (Fig. 3f). HGF injection immediately after operation was proven to be most effective (Fig. 3g).

We have developed a new experimental intestinal adhesion model. We can use bipolar forceps, which we routinely use in human surgery, to induce intestinal adhesion mimicking human intestinal adhesion. We can control the duration and intensity of cauterization by changing the mode, allowing us to treat the mice with identical invasive maneuvers in terms of quantity and quality. The procedure is simple and very straightforward, and the obtained results are very reproducible.

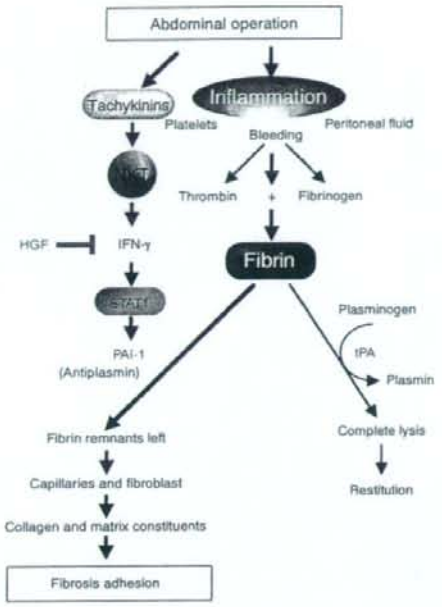

Figure 4 Causative role of NKT cell IFN-g production in induction of postsurgical adhesion formation. The balance between fibrin deposition and fibrin degradation regulates fibrous tissue formation when adhesion formation is experimentally decreased or increased by inhibition of PAI-1 or tPA, respectively. After abdominal operation, NKT cell–derived IFN-g increases the ratio of PAI-1 to tPA by activation of a STAT1-dependent pathway, leading to intestinal adhesion. A single injection of HGF protein completely inhibits intestinal adhesions by downregulation of IFN-g–dependent PAI-1 induction, providing a new potential therapeutic for the prevention of postoperative adhesions.

Other researchers have established the cecal abrasion model, the development of which depends on an IL-12–STAT4–T_H1 system[15]. In contrast, as we report here, cecal cauterization induces intestinal adhesion in an IFN-g–STAT1–NKT cell–dependent manner. In Supplementary Table 2 online, we show the features of our cauterization method and the cecal abrasion method[15]. Our adhesion model is clearly non-T_H1 and non–LPS-induced.

Our present results strongly indicate that induction of abdominal adhesion is principally dependent on endogenous IFN-g (Fig. 1b,c). NKT cells rapidly accumulate in the cecum after cauterization and express IFN-g mRNA at 3 h after treatment (Fig. 2a,e). Furthermore, **Tac1**$^{-/-}$ mice lacking tachykinins have a lower adhesion score and lower IFN-g mRNA levels (Supplementary Fig. 3), suggesting that tachykinins, including substance P, neurokinin A and neuropeptide K, induce NKT cell IFN-g production in vivo CD4$^+$ T cells from wild-type mice, but not from NKT cell–deficient mice, produce IFN-g in response to substance P, neurokinin A and neuropeptide K (Supplementary Fig. 3c).

Fibrin is important for blood clotting. If there is insufficient fibrinolytic activity, organization of the fibrin matrix and cellular and vascular ingrowths ensue, leading to fibrous bands between organs (Fig. 4)[1–3]. Here, we demonstrate that IFN-g is important for induction of PAI-1, because both **Ifng**$^{-/-}$ and **Stat1**$^{-/-}$ mice did not increase expression of PAI-1 mRNA (Fig. 3c). Thus, IFN-g is very important for induction of PAI-1 mRNA, intestinal adhesion formation and blood clotting.

Finally, we demonstrate that HGF strongly prevents intestinal adhesion by inhibiting IFN-g and PAI-1 mRNA expression in the cecum (Fig. 3f). A single injection of IFN-g–specific antibody 1 d before operation effectively inhibits abdominal adhesion (Fig. 3d). Thus, inhibition of immediate IFN-g production after surgical treatment is crucial. Although HGF has many healing effects on the gastrointestinal tract[28], our present data strongly suggest that HGF inhibits intestinal adhesion principally by suppressing rapid IFN-g production after surgical treatment. Additionally, though, the possibility of HGF-associated carcinogenicity has not been completely excluded[28]. But because of the single injection of HGF and its short half-life in the human body, HGF injection seems to be safer than HGF gene therapy, in which HGF is constitutively expressed within a limited area. Recombinant human HGF is already available for people with fatal liver disease; the results presented here strongly indicate that HGF treatment can be a new strategy for prevention of postsurgical adhesion formation.

IFN-g is a very crucial cytokine for host defense. Therefore, careful co-administration of antibiotics might be important during modulation of IFN-g by our approach. HGF treatment seems to be a promising way for preventing adhesion without affecting anastomoses of cut ends of bowel, because this treatment shows healing effects on the gastrointestinal tract. Of course, extensive basic studies are needed to estimate the translational potential of HGF treatment for the prevention of intestinal adhesion formation in human cases.

METHODS

Mice. We purchased BALB/c, C57BL/6 (B6), B6 **Tac1**$^{-/-}$, BALB/c **Stat6**$^{-/-}$, C3H/HeN and C3H/HeJ mice from Jackson Laboratory. We bred BALB/c NKT cell–deficient, BALB/c **Ifng**$^{-/-}$, B6 **Il12p40**$^{-/-}$, B6 **Il18**$^{-/-}$, B6 **Myd88**$^{-/-}$, B6 **Tnfa**$^{-/-}$ mice under specific pathogen–free conditions at the animal facilities of Hyogo College of Medicine. We bred BALB/c **Stat4**$^{-/-}$ and 129/Sv **Stat1**$^{-/-}$ mice under specific pathogen–free conditions in the animal facilities at Tokyo Medical University. All animal experiments were performed in accordance with the guidelines of the Institutional Animal Care Committee, Hyogo College of Medicine and Tokyo Medical University.

Mouse model of surgical adhesion formation. We anesthetized mice with 0.15 ml (20% vol/vol) diluted pentobarbital sodium solution (10 mg/ml). We made an anterior midline incision through the abdominal wall and peritoneum. We isolated the cecum and cauterized it using the coagulation mode of bipolar forceps (MERA; 30 W, 500 kHz, 150 O) for one second. We closed the incision in two layers with silk sutures. Daily histological examination revealed that this surgical treatment did not induce penetration of the intestinal wall, suggesting that the burned site did not induce an influx of bacteria from lumen into peritoneal cavity. We killed the mice 7 d later, when they were examined by an observer blinded to the identity of the experimental groups. Each mouse was evaluated according to the following standard scoring system, which has been widely used in this field[15,29,30]: score 0, no adhesion; score 1, one thin filmy adhesion; score 2, more than one thin adhesion; score 3, thick adhesion with focal point; score 4, thick adhesion with plantar attachment or more than one thick adhesion with focal point; and score 5, very thick vascularized adhesion or more than one plantar adhesion.

Reagents. We purchased recombinant mouse IFN-g and HGF from Genetics Institute and Peprotech, respectively.

In vivo treatment of mice. For adoptive CD4$^+$ T cell transfer experiments, we purified splenic CD4$^+$ T cells from wild-type or **Ifng**$^{-/-}$ mice with MicroBeads (antibody to mouse CD4; clone RM4-5, Miltenyi Biotec). We transferred CD4$^+$ T cells to NKT cell–deficient mice (1.0 10^7 cells per mouse) via the tail vein route 7 d before surgery. For treatment with IFN-g, we subcutaneously infused osmotic pumps (DURECT) filled with IFN-g (100 mg) in 100 ml PBS into mice

2 d before surgery. The pumping rate of an osmotic pump was 0.5 ml/h continuously, and the duration was 7 d. We subcutaneously injected mice with HGF (0, 5, 10 or 20 mg per mouse) in 200 ml of PBS on the days indicated in Figure 3g before or after surgery. The detailed protocols of antibody treatment to deplete $CD4^+$ T cells and IFN-g are described in the Supplementary Methods online.

Histology. We fixed tissues in 10% buffered formalin, embedded them in paraffin, cut them into 3-mm sections and stained them with H&E or picric acid and Sirius red.

Quantitative reverse transcription PCR. We extracted total RNA from the cecum with the RNeasy Plus Mini Kit (QIAGEN) and synthesized the cDNA using SuperScript III RNase H^- Reverse Transcriptase (Invitrogen). We quantified the expression of the gene with TaqMan Gene Expression Assays (Applied Biosystems). We expressed the results as relative expression standardized with the expression of the gene encoding eukaryotic 18S ribosomal RNA. Specific primers used for quantitative RT-PCR are described in the Supplementary Methods.

Enzyme-linked immunosorbent assay. We measured the abundance of PAI-1 and tPA in plasma with a mouse PAI-1 ELISA kit (Innovative Research) and mouse tPA ELISA kit (Oxford Biomedical Research), respectively.

Statistical analyses. Data are given as means ± s.e.m. We made statistical comparisons between two experimental groups by Student's paired t-test performed with GraphPad Instat Software. We considered a P value o0.05 as significantly different.

Note: Supplementary information is available on the Nature Medicine website.

ACKNOWLEDGMENTS

This study was supported by a Grant-in-Aid for Scientific Research on Priority Areas and a Hitech Research Center grant from the Ministry of Education, Culture, Sports, Science and Technology of Japan and a Grant-in-Aid for Scientific Research (B; No. 19390342) from the Japan Society for Promotion of Science.

AUTHOR CONTRIBUTIONS

Tomohiro Yoshimoto and K.N. formulated the hypothesis and initiated and organized the study; H.K. and Tomohiro Yoshimoto performed the main experimental work and analyzed the data; Takayuki Yoshimoto helped with some experimental procedures; Tomohiro Yoshimoto and K.N. oversaw the experiments, analyzed the data and provided the main funding for the research; J.F. contributed to data discussion; Tomohiro Yoshimoto drafted the manuscript and K.N. prepared the final manuscript.

Published online at http://www.nature.com/naturemedicine
Reprints and permissions information is available online at http://npg.nature.com/reprintsandpermissions

1. Holmdahl, L. The role of fibrinolysis in adhesion formation. Eur. J. Surg. 163 (Suppl. 577), 24–31 (1997).
2. Raftery, A.T. Regeneration of peritoneum: a fibrinolytic study. J. Anat. 129, 659–664 (1979).
3. Sulaiman, H., Dawson, L., Laurent, G.J., Bellingan, G.J. & Herrick, S.E. Role of plasminogen activators in peritoneal adhesion formation. Biochem. Soc. Trans. 30, 126–131 (2002).
4. Holmdahl, L. & Ivarsson, M.L. The role of cytokines, coagulation, and fibrinolysis in peritoneal tissue repair. Eur. J. Surg. 165, 1012–1109 (1999).
5. Fanciullacci, M., Fedi, S., Alessandri, M. & Pietrini, U. Substance P-induced fibrinolysis in the forearm of healthy humans. Experientia 49, 242–244 (1993).
6. Reed, K.L. et al. Neurokinin-1 receptor and substance P messenger RNA levels increase during intraabdominal adhesion formation. J. Surg. Res. 108, 165–172 (2002).
7. Reed, K.L. et al. A neurokinin 1 receptor antagonist decreases postoperative peritoneal adhesion formation and increases peritoneal fibrinolytic activity. Proc. Natl. Acad. Sci. USA 101, 9115–9120 (2004).
8. Miyazawa, K. et al. Molecular cloning and sequence analysis of cDNA for human hepatocyte growth factor. Biochem. Biophys. Res. Commun. 163, 967–973 (1989).
9. Nakamura, T. et al. Molecular cloning and expression of human hepatocyte growth factor. Nature 342, 440–443 (1989).
10. Ellis, H. The clinical significance of adhesions: focus on intestinal obstruction. Eur. J. Surg. 163 (Suppl. 577), 5–9 (1997).
11. Ellis, H. et al. Adhesion-related hospital readmissions after abdominal and pelvic surgery: a retrospective cohort study. Lancet 353, 1476–1480 (1999).
12. Menzies, D. & Ellis, H. Intestinal obstruction from adhesions–how big is the problem? Ann. R. Coll. Surg. Engl. 72, 60–63 (1990).
13. Parker, M.C. et al. Colorectal surgery: the risk and burden of adhesion-related complications. Colorectal Dis. 6, 506–511 (2004).
14. Ghellai, A.M. et al. Role of transforming growth factor-b1 in peritonitis-induced adhesions. J. Gastrointest. Surg. 4, 316–323 (2000).
15. Chung, D.R. et al. $CD4^+$ T cells regulate surgical and postinfectious adhesion formation. J. Exp. Med. 195, 1471–1478 (2002).
16. Bendelac, A., Savage, P.B. & Teyton, L. The biology of NKT cells. Annu. Rev. Immunol. 25, 297–336 (2007).
17. Taniguchi, M., Harada, M., Kojo, S., Nakayama, T. & Wakao, H. The regulatory role of Va14 NKT cells in innate and acquired immune response. Annu. Rev. Immunol. 21, 483–513 (2003).
18. Yoshimoto, T. & Paul, W.E. $CD4^{pos}$, $NK1.1^{pos}$ T cells promptly produce interleukin 4 in response to in vivo challenge with anti-CD3. J. Exp. Med. 179, 1285–1295 (1994).
19. Cui, J. et al. Requirement for Va14 NKT cells in IL-12–mediated rejection of tumors. Science 278, 1623–1626 (1997).
20. Meraz, M.A. et al. Targeted disruption of the Stat1 gene in mice reveals unexpected physiologic specificity in the JAK-STAT signaling pathway. Cell 84, 431–442 (1996).
21. Kawano, T. et al. Natural killer–like nonspecific tumor cell lysis mediated by specific ligand-activated Va14 NKT cells. Proc. Natl. Acad. Sci. USA 95, 5690–5693 (1998).
22. Kaplan, M.H., Sun, Y.L., Hoey, T. & Grusby, M.J. Impaired IL-12 responses and enhanced development of T_H2 cells in Stat4-deficient mice. Nature 382, 174–177 (1996).
23. Takeda, K. et al. Essential role of Stat6 in IL-4 signalling. Nature 380, 627–630 (1996).
24. Katayama, I. & Nishioka, K. Substance P augments fibrogenic cytokine-induced fibroblast proliferation: possible involvement of neuropeptide in tissue fibrosis. J. Dermatol. Sci. 15, 201–206 (1997).
25. Zimmer, A. et al. Hypoalgesia in mice with a targeted deletion of the tachykinin 1 gene. Proc. Natl. Acad. Sci. USA 95, 2630–2635 (1998).
26. Holmdahl, L., Eriksson, E., al-Jabreen, M. & Risberg, B. Fibrinolysis in human peritoneum during operation. Surgery 119, 701–705 (1996).
27. Kuroiwa, T. et al. Hepatocyte growth factor ameliorates acute graft-versus-host disease and promotes hematopoietic function. J. Clin. Invest. 107, 1365–1373 (2001).
28. Ido, A., Numata, M., Kodama, M. & Tsubouchi, H. Mucosal repair and growth factors: recombinant human hepatocyte growth factor as an innovative therapy for inflammatory bowel disease. J. Gastroenterol. 40, 925–931 (2005).
29. Kennedy, R., Costain, D.J., McAlister, V.C. & Lee, T.D. Prevention of experimental postoperative peritoneal adhesions by N,O-carboxymethyl chitosan. Surgery 120, 866–870 (1996).
30. Kocak, I., Unlu, C., Akcan, Y. & Yakin, K. Reduction of adhesion formation with cross-linked hyaluronic acid after peritoneal surgery in rats. Fertil. Steril. 72, 873–878 (1999).

Journal of Dermatological Science (2008) 51, 19–29

ELSEVIER

Dermatological SCIENCE

www.intl.elsevierhealth.com/journals/jods

Freshly isolated Langerhans cells negatively regulate naïve T cell activation in response to peptide antigen through cell-to-cell contact

Yasutomo Imai [a,b], Nobuki Hayashi [b], Koubun Yasuda [b], Hiroko Tsutsui [c], Hitoshi Mizutani [a], Kenji Nakanishi [b,*]

[a] Department of Dermatology, Mie University School of Medicine, Tsu 514-8507, Japan
[b] Department of Immunology & Medical Zoology, Hyogo College of Medicine, 1-1 Mukogawa-cho, Nishinomiya 663-8501, Japan
[c] Department of Microbiology, Hyogo College of Medicine, 1-1 Mukogawa-cho, Nishinomiya 663-8501, Japan

Received 3 December 2007; received in revised form 10 January 2008; accepted 16 January 2008

KEYWORDS
Langerhans cells;
T cell activation;
Cell division;
Mouse

Summary

Background: Epidermal Langerhans cells (LCs) have been believed to function as professional antigen-presenting cells (APCs). However, LC-ablated mice reportedly suffer from severer contact hypersensitivity (CHS) upon cutaneous challenge with hapten than wild-type mice, suggesting LCs as regulators of adaptive immune responses in the skin.
Objective: This study was designed to address the possible regulatory roles of LCs in the balanced primary adaptive immune responses to protein antigens.
Methods: LCs were freshly isolated from skin of BALB/c mice (>95% positive for MHC class II). Naïve $CD4^+$ T cells reactive to ovalbumin (OVA) were purified by FACS-sorting from lymph node cells of DO11.10 BALB/c mice, labeled with CSFE, and incubated with OVA peptide in the presence of splenic dendritic cells (DCs) and/or LCs. Cell division frequencies were determined by the degree of serially diluted expressions of CSFE in the individual $CD4^+$ T cells.
Results: Approximately 70% of them underwent cell division when naïve $CD4^+$ T cells were activated by OVA presented by splenic DCs. In contrast, LCs only very modestly induced their cell division. Furthermore, LCs inhibited the cell division induced by splenic DCs, and this regulatory action was abolished by prevention of their contact to other cells, but not by the treatment with neutralizing antibodies against IL-10 or TGF-b, well-established regulatory cytokines.

* Corresponding author. Tel.: +81 798 45 6572; fax: +81 798 40 5423.
E-mail address: nakaken@hyo-med.ac.jp (K. Nakanishi).

0923-1811/$30.00 # 2008 Japanese Society for Investigative Dermatology.
doi:10.1016/j.jdermsci.2008.01.005

Conclusion: LCs negatively regulate the primary adaptive T cell response, presumably allowing well-controlled immune response in the skin.

1. Introduction

Epidermal Langerhans cells (LCs) have been extensively examined for their biological properties since their discovery in 1868 [1]. Naïve $CD4^+$ T cells require two important signals to be successfully activated. One is induced by antigen (Ag) recognition by T cell receptor complex in the context of MHC class II proteins expressed on professional Ag-presenting cells (APCs) named as dendritic cells (DCs), and the other is provided by the interaction of CD28 with costimulators, CD80/CD86, on the professional APCs [1]. Since they express those surface proteins as well, LCs have been believed to play an important role in the development of adaptive immune responses as professional APCs during cutaneous challenge with pathogens and allergens [2–4]. Recently, a third T cell activation signal was demonstrated to be critical for naïve $CD4^+$ T cell activation, particularly for their Th1 cell differentiation [5–7]. DCs produce IL-12, a prototype Th1-driving cytokine, in response to microbial products via their pattern recognition receptors including Toll-like receptors (TLRs). However, it is intriguingly to note that LCs poorly produce IL-12 upon TLR engagement despite expressing substantial levels of TLRs [2], suggesting that LCs might have insufficient capacity to activate naïve T cells. Therefore, it is important to know whether highly purified LCs are capable of activating the cellular immune responses.

Accumulated lines of evidence implicate that DCs are highly heterogeneous in phenotypes and biological actions, but can be basically divided into two functional subsets, immunogenic DCs and regulatory DCs [8–10]. The immunogenic DCs contribute to driving Ag-specific T cell responses via providing those three signals [5,6,11]. The regulatory DCs can evoke both peripheral deletion or negative regulation of self-Ag-reactive T cells for establishing peripheral T cell tolerance and induction of foreign Ag-specific regulatory T cells (Treg) for protecting pathological responses, particularly in the sites segregating the insides from the outsides, such as respiratory tract, intestinal mucosa, and perhaps skin [8,10,12]. It is believed that DCs might play either immunogenic or tolerogenic roles depending on the intrinsic features of and environmental properties around the DCs but not on the cell lineage of the DCs [10], prompting us to perform analyses of LC functions.

Recent reports suggest poor contribution of LCs to the accomplishment of cellular immune responses upon cutaneous challenge with hapten. Knock-in mice that express GFP under the control of the gene for langerin, that is a C-type lectin selectively expressed on LCs but not other DCs, revealed late onset migration of LCs into the regional lymph nodes (LNs) after cutaneous application of Ag, implicating dispensability of LCs in the development of Ag-specific adaptive immune responses [13,14]. It was also clearly demonstrated that LC-abrogated mice exhibit normal or exacerbated contact hypersensitivity (CHS) response to topically applied hapten [13,15], suggesting that LCs might rather negatively regulate adaptive immune response. Here, we investigated whether and how LCs control the development of primary T cell response to protein Ag. We prepared freshly isolated LC population with high purity (>95%) by FACS-sorting and compared their exogenous Ag-presenting activity with the conventional DCs purified from splenocytes. To test this ability, we used highly purified naïve $CD4^+$ LN T cells from mice transgenic for the TCR ab recognizing ovalbumin (OVA), $OVA_{323–339}$ peptide in accuracy. LCs, unlike splenic DCs, poorly induce proliferative response of naïve OVA-specific $CD4^+$ T cells. Furthermore, LCs could cell number-dependently inhibit their proliferative response to the OVA peptide presented by splenic DCs. These results suggest that LCs play an important role as negative regulators to tip a balance of adaptive immune responses to foreign proteins and/or presumably to induce peripheral T cell tolerance to self-proteins. Our present results would provide a new insight into the cutaneous immune diseases due to allergic and autoimmune disorders.

2. Materials and methods

2.1. Animals

BALB/c female mice, 6–10 weeks of age, were purchased from Oriental Yeast (Osaka). Transgenic BALB/c mice named as DO11.10 mice, whose $CD4^+$ T cells express ab TCR recognizing $OVA_{323–339}$ [16], were kindly provided by D. Loh at Washington University (St. Louis, MO). All mice were kept under specific pathogen-free conditions and received

humane care as outlined in the Guide for the Care and Use of Experimental Animals in Hyogo College of Medicine, which is based on the Guide for the Care and Use of Laboratory Animals in Institute of Laboratory Animal Resources, National Research Council (1996).

2.2. Reagents

Anti-CD28, anti-CD3, anti-FcgR, anti-CD4, anti-CD8, anti-CD11c, anti-CD44, anti-CD62L, anti-CD69, anti-B220, anti-DX5, and anti-MHC class II ($I\text{-}A^d$) monoclonal antibodies (mAbs) were purchased from PharMingen (San Diego, CA). Anti-CD80 and anti-CD86 mAbs were from BioLegend (San Diego, CA). Anti-langerin polyclonal Abs (goat IgG, Santa Cruz Biotechnology, Santa Cruz, CA) that recognize cytoplasmic portion of mouse langerin and FITC-conjugated anti-goat IgG Abs (Santa Cruz Biotechnology) were used for cytoplasmic staining of mouse langerin [13,15]. Purified neutralizing rat anti-mouse IL-10 mAb was purchased from Becton Dickinson (San Jose, CA). Neutralizing mAb against anti-TGF-b1, -b2, and -b3 was from R&D Systems (Minneapolis, MN). $OVA_{323-339}$ peptide was purchased from ANASPEC (San Jose, CA). The culture medium generally used in this study was RPMI 1640 supplemented with 10% heat-inactivated fetal calf serum, 50 mM 2-ME, 2 mM L-glutamine, 100 U/ml penicillin, and 100 mg/ml streptomycin.

2.3. Preparation of LCs

LC-including epidermal cell suspension was prepared according to the method described previously with some modifications [17]. LCs were then selectively collected using the automated cell sorter and had a purity of over 95% [18]. Briefly, pieces of mouse ear and trunk skin were incubated with DISPASE II (3000U, Godo Shusei, Tokyo, Japan) for 50 min at 37 8C in a dish with 10 cm diameter. Epidermis was peeled off and incubated in fresh culture medium containing 0.025% DNase I (Roche, Mannheim, Germany) for 15 min at 37 8C. An epidermal cell suspension was obtained after vigorously pipetting the epidermal sheets, and cells were centrifuged on a discontinuous 30–60% Percoll density gradient (two layers: 30 and 60%). Cells at the 30–60% interface were collected and incubated with PE- or FITC-anti-$I\text{-}A^d$ mAb. $I\text{-}A^{d\ high}$ cells were purified by electronic cell sorting using a FACSAria Cell Sorter (Becton Dickinson) with according to the manufacturer's instructions. The LC purity was examined by FACS analysis, and the LC preparations with more than 95% for $I\text{-}A^d$ were used.

2.4. Preparation of splenic DCs

Spleens were perfused with RPMI 1640 supplemented with 0.5 mg/ml of collagenase (Roche), and the cell suspensions were further digested with 0.5 mg/ml of collagenase for 20 min at 37 8C, followed by subsequent pressing the undigested pieces through cell strainers (Falcon Labware, Oxnard, CA). The cells were collected, and erythrocytes were lysed by incubating the cells with ammonium-chloride lysing buffer (155 mM NH_4Cl, 10 mM $KHCO_3$ and 100 mM EDTA-2Na/$2H_2O$) for 1 min on ice. $CD11c^{high}$ DCs were separated by positive magnetic selection using microbeads-conjugated anti-mouse CD11c (Miltenyi Biotec, Belgisch Gladbach, Germany) and a magnetic cell separator (AutoMACS$^{\text{I}}$) according to the manufacturer's instructions. The MACS-sorted cells were, then, stained with PE-conjugated anti-CD11c and FITC-conjugated anti-$I\text{-}A^d$, or FITC-conjugated anti-CD11c and allophycocyanine (APC)-conjugated anti-$I\text{-}A^d$, and $CD11c^{high}$ $I\text{-}A^{d\ high}$ cells were further purified by the FACS-sorting using a FACSAria Cell Sorter. The DC preparations with purity more than 98% for CD11c determined by FACS were used.

2.5. Preparation of splenic B cells

B cells were isolated from erythrocyte-lysed splenocytes of BALB/c mice by negative selection, using FITC-conjugated mAbs against CD3, CD4, CD8, CD11c and DX5 followed by incubation with magnetic beads coated with anti-FITC Abs (Miltenyi Biotec). The cells were then stained with FITC-anti-$I\text{-}A^d$, APC-anti-CD11c and PE-anti-B220, and $I\text{-}A^{d\ +}B220^+CD11c$ cells were further purified by the FACS-sorting using a FACSAria Cell Sorter. The cell preparations with purity more than 98% for B220 determined by FACS were used.

2.6. Preparation of Naïve $CD4^+$ T cells

$CD4^+$ T cells were isolated from axillary, inguinal, and mesenteric LNs of DO11.10 mice by negative selection, using FITC-conjugated mAbs against B220, CD8, DX5, CD11c, and $I\text{-}A^d$ followed by incubation with anti-FITC Ab-coated magnetic beads [19,20]. The cell preparations with purity more than 99% for CD4 were used. The cells were then stained with PE-anti-62L and FITC-anti-CD44 mAbs. $CD62L^{high}$ $CD44^{low}$ naïve T cells were further purified by the FACS-sorting using a FACSAria Cell Sorter.

2.7. FACS analysis

Fluorescence-staining of cells was performed after treatment with anti-FcgR mAb at least 20 min.

Fluorescence-staining of cell surface proteins were performed according to the methods described previously [20]. Co-expression of langerin of FACS-sorted I-$A^{d\ high}$ LCs was examined by cytoplasmic staining of langerin, because the Abs used recognize cytoplasmic portion of mouse langerin. Briefly, FACS-sorted I-$A^{d\ high}$ cells were fixed and permeabilized with a kit (PharMingen) [20], and stained in sequence with anti-langerin Abs or control goat IgG and FITC-anti-goat IgG (PharMingen). FACS-sorted LCs after staining with FITC-anti-I-A^d were further stained with PE-anti-CD80 or PE-anti-CD86. FASC-sorted splenic DCs after staining with FITC-anti-I-A^d were stained with PE-anti-CD80 and PE-anti-CD86. FACS-sorted naive $CD4^+$ T cells were stained with FITC-anti-CD44 and APC-anti-CD4. CSFE-labeled naive $CD4^+$ T cells following activation with various protocols were stained with PE-anti-CD69. Phenotypes of those cells were examined by a FACScalibur followed by analyses with CellQuest software (Becton Dickinson).

2.8. Confocal laser microscopic analysis

LCs stained with PE-anti-I-A^d and FITC-anti-langerin were spun onto a slide glass by using Cytospin[1], and the subcellular localization of I-A^d and langerin was analyzed by confocal laser microscopy (Model IX81, Olympus, Tokyo Japan).

2.9. CFSE labeling

Naïve $CD4^+$ T cells were washed twice in PBS and resuspended in PBS at a concentration of 2–3 10^7 cells/ml. The cells were added with an equal volume of freshly diluted 1.25 mM CFSE in PBS (Molecular Probes, Eugene, OR) and incubated for 4 min at room temperature. The reaction was stopped by the addition of an equal volume of FCS [19,20]. The cells were immediately washed three times with the culture medium.

2.10. In vitro T cell activation assay

1 10^6 cells/ml of CFSE-labeled naive $CD4^+$ T cells were incubated with 1 mM of OVA peptide in the presence of fixed cell number of splenic DCs (1 10^5 ml^{-1}) and/or LCs or splenic B cells at various LC/DC or B cell/DC ratios in a 96-well plate with flat bottoms. In some experiments CFSE-labeled naïve $CD4^+$ DO11.10 T cells were incubated with 1 mM of OVA peptide in the presence of 1 10^5 ml^{-1} of splenic DCs and 2 10^5 ml^{-1} of LCs with or without neutralizing anti-IL-10 or neutralizing anti-TGF-b [21]. The neutralizing anti-IL-10 Ab (1 mg/ml) and anti-TGF-b Ab (0.5 mg/ml) used in this study can inhibit 50% of bioactivity of at least 15 ng/ml of rIL-10 and 10 ng/ml of rTGF-b1, respectively, both of which are pharmacological doses, according to the manufacture's data sheets. In some experiments LCs were separately incubated with the naïve $CD4^+$ T cells and splenic DCs by using BD Falcon 96-Multiwell Insert System (Becton Dickinson). LCs were added in the inner wells, and the other cell preparations together with OVA peptide were in the outer wells. After 72 h-culture, cells were collected and washed by PBS. Cells were stained by APC-labeled anti-CD4 and PE-labeled anti-CD69. Proliferative response of the $CD4^+$ T cells was determined by the following formula. Cells once divided showed a half of the CSFE intensity on parental cells. We calculated each cell number of cells with no cell division, and cells with one, two, and three cycles of cell division. Cell division percentage (%) = 100 ($CD4^+$ T cell number with 1–3 cycles of cell division)/($CD4^+$ T cell number with 0–3 cycles of cell division). In some experiments, we incubated naïve $CD4^+$ T cells and OVA peptide plus splenic DCs in the presence and absence of LCs at various LC/DC ratios and evaluated the regulatory effect of the additional LCs by calculating the percent inhibition as follows:

$$\text{percent inhibition} = 100 \left(1 - \frac{\text{the cell division percentage in the presence of LCs}}{\text{the cell division percentage in the absence of LCs}} \right)$$

2.11. Statistics

All experiments were repeated at least twice with similar results. The results displayed in the figures are representative of three or more independent experiments with similar results.

3. Results

3.1. Robust expressions of MHC class II and langerin on freshly isolated and highly purified LCs

To examine biological functions of LCs we prepared freshly isolated LCs with high purity. I-A positive cells were FACS-sorted from epidermal cell suspension of BALB/c mice. More than 95% cells were positive for I-A^d (Fig. 1A). Cytoplasmic staining for langerin revealed that more than 95% I-A^+ cells express langerin protein as well (Fig. 1B). The I-A^+ cells expressed both CD80 and CD86 at high intensity on their surface (Fig. 1F, lower panels). Moreover,

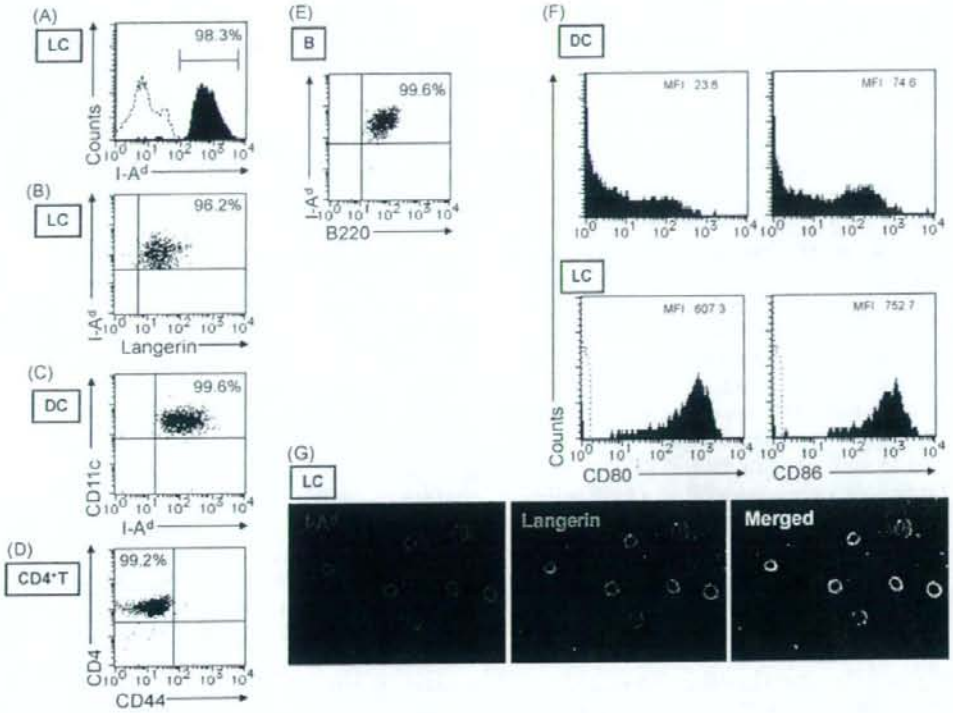

Fig. 1 Freshly isolated LCs obviously express costimulators as well as MHC class II. Freshly isolated LCs shown as LC were prepared using the automated cell sorter and examined for surface expressions of I-A^d (A) and CD80 or CD86 (F), and for surface I-A^d in combination with cytoplasmic langerin (B and G). Splenic DCs (DC) prepared were examined for surface CD11c and I-A^d (C) and CD80 or CD86 (F). Naïve CD4$^+$ LN Tcells (CD4$^+$ T) were isolated from DO11.10 mice and examined for their surface expressions of CD4 and CD44 (D). Splenic B cells (B) were examined for their surface expression of I-A^d as well as B220 (E). The representative data are shown. The similar results were obtained in separate three experiments.

we examined morphological and phenotypical aspects of the sorted cells by confocal laser microscopic analysis and found that most of the cells had DC-like morphology and were positive for both I-A^d and langerin protein (Fig. 1G). These results clearly demonstrated that the epidermal I-A$^+$ cell preparation has the characteristics associated with LCs. Thus, we used this cell preparation as freshly isolated LCs in this study.

3.2. LC expression of high levels of costimulators

Next, we compared cell surface expressions of costimulators between LCs and conventional DCs. Since splenic DCs are well established conventional DCs [9], we isolated CD11c$^+$ spleen cells. Almost all CD11c$^+$ cells co-expressed I-A^d (Fig. 1C). The intensity of I-A^d of LCs was comparable as splenic DCs (Fig. 1A and C), suggesting that the LCs might serve as APCs. Mean fluorescence intensity (MFI) of CD80 and CD86 were 23.6 and 74.6, respectively, in splenic DC (Fig. 1G, upper panels). LCs expressed much higher MFI of both costimulators as compared to splenic DCs (Fig. 1G, lower panels), strengthening the LCs as professional APCs. Based on those surface phenotypes LCs appeared to possess professional APC activity at least equivalent to splenic DCs.

3.3. Poor APC activity of LCs onto naïve CD4$^+$ T cells

Next, we investigated whether LCs, like splenic DCs, are capable of activating naïve CD4$^+$ Tcells. For this we manipulated DO11.10 BALB/c mice, whose CD4$^+$ T cells selectively express the TCR ab recognizing the OVA peptide. LN cells of DO11.10 mice were incubated with mAb mixture against CD8, CD11c, DX5, B220, and I-A molecules, and CD4$^+$ Tcells were negatively selected by AutoMACS[1]. CD62L^{high} CD44^{low} naïve cells were further purified by FACS-sorting. As more than 99% of the sorted cells were CD4$^+$CD44^{low} (Fig. 1D), we used this cell population as naïve CD4$^+$ T cells. Professional APC activity was

determined by the induction of cell division of the naïve CD4+ T cells in response to the OVA peptide. We labeled these naïve CD4+ T cells with CSFE and incubated them with the OVA peptide in the presence of freshly isolated LCs or splenic DCs. At day 3, the cells were harvested and examined for expression of CSFE. Consistent with our previous report [20], more than 75% of the cells expressed CD69, a pan-activation marker. The CD69+cells showed obvious cell division, while all the CD69 cells remained undivided (Fig. 2, upper panel). In sharp contrast to splenic DCs, LCs could not activate the naïve CD4+ DO11.10 T cells to express CD69 or induce their cell division (Fig. 2, lower panel). Thus, in contrast to splenic DCs, LCs could not activate naïve CD4+ cells at all. These results clearly demonstrated

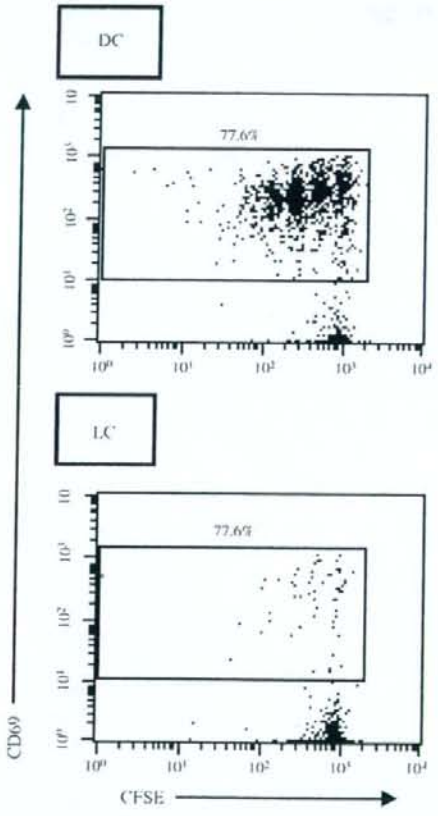

Fig. 2 LCs, unlike splenic DCs, fail to activate naïve CD4+ T cells. Naïve CD4+ LN T cells from DO11.10 mice were labeled with CSFE, and the CSFE-labeled cells (1 10^6 ml $^{-1}$) were incubated with OVA peptide in the presence of 1 10^5 ml $^{-1}$ of splenic DCs (upper panel) or of LCs (lower panel) for 3 days. Cells were collected and analyzed for levels of CSFE and CD69 gated on the CD4+ cells. The representative data are shown. The similar results were obtained in separate three experiments.

that freshly isolated LCs, although outstandingly expressing costimulators and MHC class II, possess poor professional APC activity.

3.4. LCs negatively regulate splenic DC induction of naïve CD4+ T cell activation

LC-ablated mice showed severer CHS than WT mice [15], prompting us to investigate whether LCs suppress splenic DC induction of naïve CD4+ T cell activation. We incubated CSFE-labeled naïve CD4+ T cells with the OVA peptide plus a fixed cell number of splenic DCs in the presence of various cell numbers of LCs shown by the LC/DC ration and examined cell divisions of the CD4+ T cells. When the naïve CD4+ T cells were incubated with OVA peptide plus splenic DCs in the absence of LCs, more than 70% cells underwent cell division (Fig. 3, left panel). This is consistent with the above result (Fig. 2, upper panel). Consistent with the above result (Fig. 2, lower panel), the cell division percentage was only 10% when the naïve CD4+ T cells were incubated with OVA peptide and LCs in the absence of splenic DCs (Fig. 3, right panel). When the naïve CD4+ T cells were primed with the peptide plus splenic DCs but supplemented with the same number of LCs as splenic DCs, only 60% of the CD4+ T cells showed cell division (Fig. 3, third panel from the left-hand side). Furthermore, the more numbers of LCs were added, the less percentage of the CD4+ T cells underwent cell division (Fig. 3A). Indeed, percent inhibition was increased in a LC/DC ratio-dependent manner (Fig. 3A). These results suggested that LCs might negatively regulate splenic DC-induced naïve cell activation.

The apparent inhibitory action of LCs on the DC activation of naïve T cells, however, might be simply due to LC competing with splenic DCs for the TCR. To exclude this possibility we conducted experiments whether freshly isolated B cells are able to diminish the DC activation of T cells, because B cells, like LCs, express MHC class II and have weak capacity to fully activate naïve T cells [22]. Indeed, splenic B cells expressed comparable levels of I-A^d as did freshly isolated LCs (Fig. 1E). Furthermore, B cells, like LCs, failed to activate naïve CD4+ T cells (Fig. 3B, right panel). It is intriguingly to note that in contrast to LCs, B cells do entirely not reduce the percentage of divided T cells induced by splenic DCs (Fig. 3B), indicating that competition for the TCR does not simply reduce DC activation of naïve T cells. These results suggested that negative regulatory action on the DC-induced naïve T cell activation is a unique feature of freshly isolated LCs. Taken together these results demonstrated that LCs negatively regulate professional APC-induced naïve CD4+ T cell activation in a cell number ratio-dependent manner.

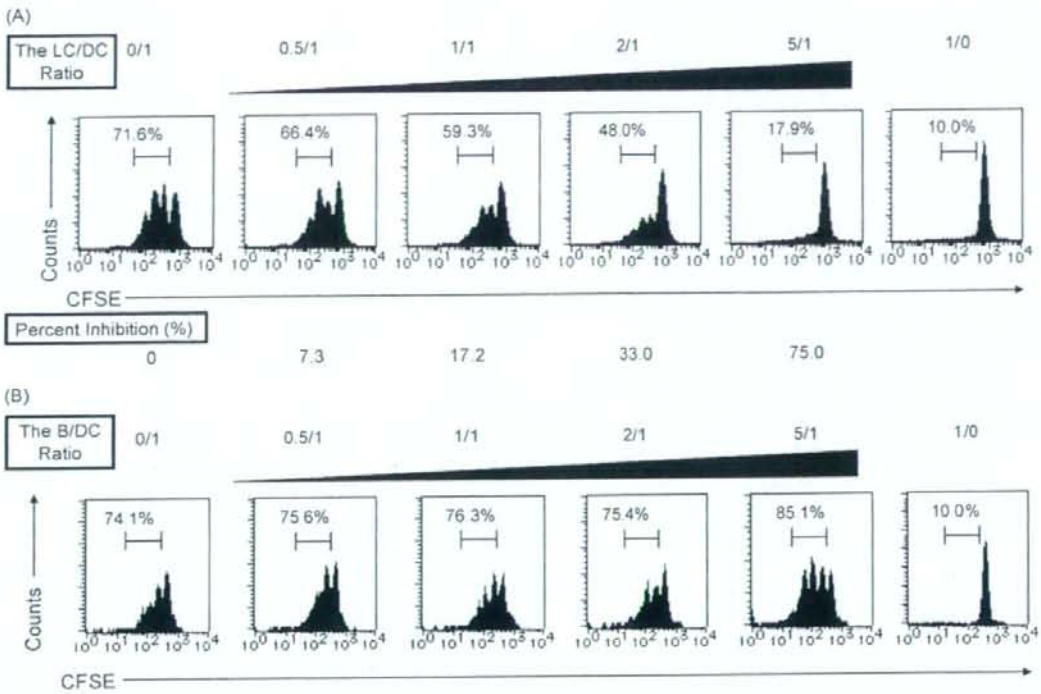

Fig. 3 LCs negatively regulate naïve T cell activation. CSFE-labeled naïve $CD4^+$ T cells prepared from DO11.10 mice (1 10^6 ml $^{-1}$) were incubated with OVA peptide and splenic DCs (1 10^5 ml $^{-1}$) in the presence or absence of LCs (A) or B cells (B) at various LC/DC or B cell/DC (B/D) ratios. The LC/DC and B/DC ratio 1/0 indicates that only 1 10^5 ml $^{-1}$ of LCs or B cells were added as APCs, respectively. Cells were collected and analyzed for CSFE. Proportions of $CSFE^+$ cells undergoing 1–3 cycles of cell division to those undergoing 0–3 cycles were calculated. The percent inhibitions of the added LCs were also calculated. The representative data are shown. The similar results were obtained in separate three experiments.

3.5. Requirement of cell-to-cell contact for LC regulation of T cell activation

Finally, we investigated the mechanism by which LCs inhibit the professional APC-induced naïve $CD4^+$ T cell activation. Since TGF-b and IL-10 are potent inhibitory molecules produced by LCs as well as DCs and are involved in the negative regulation of naïve T cell activation in mucosal immunity and cutaneous immune system [9,23–26], we addressed whether those molecules are important for the LC regulation of the naïve T cell activation. To test this, we incubated naïve $CD4^+$ T cells with OVA peptide together with splenic DCs and LCs at 0/1 or 2/1 of the LC/DC ratio in the presence of control Ab or neutralizing anti-TGF-b or anti-IL-10 mAb that can neutralize pharmacological doses of the corresponding cytokines. Similar to the above results (Fig. 3A), the cell division percentage was reduced from 73% to 46%, when naïve $CD4^+$ T cells were incubated in the presence of control Ab at 2/1 of the LC/DC ratio as compared to those at 0/1, indicating negligible effect of control Ab (Fig. 4A, upper panels). The percent inhibition of the LCs was 36.6%. When the $CD4^+$ T cells were cultured under the same conditions but in the presence of neutralizing anti-TGF-b mAb, the cell division percentage was similarly dampened from 73% to 50% (Fig. 4A, lower panels). The percent inhibition of the LCs was 31.8%. These results indicated a minor role of endogenous TGF-b in the LC regulation of the T cell activation. The addition of LCs decreased the cell division percentage of the $CD4^+$ T cells from 67% to 50% (percent inhibition was 25.3%) and 63% to 53% (percent inhibition was 16.7%), when the cells were incubated with control Ab and neutralizing anti-IL-10, respectively (Fig. 4B). This indicated that endogenous IL-10 is not profoundly involved in the regulatory action of the LCs. These results demonstrated that TGF-b or IL-10 is not solely essential for the negative regulation of the naïve $CD4^+$ T cell activation.

We wanted to know whether LCs require cell-to-cell contact to exert their regulatory action. We

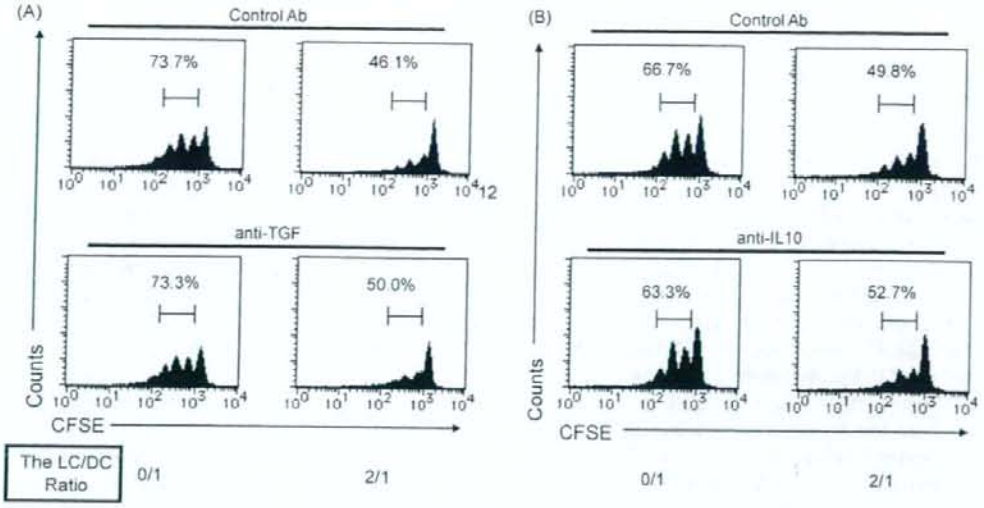

Fig. 4 Dispensability of TGF-b and IL-10 for LC regulation of naïve T cell activation CSFE-labeled naïve $CD4^+$ T cells prepared from DO11.10 mice were incubated with OVA peptide as well as splenic DCs (1 10^5 ml $^{-1}$) plus LCs (2 10^5 ml $^{-1}$) in the presence of isotype-matched control mAbs (A and B upper panels) or neutralizing anti-TGF-b (A lower panels) or anti-IL-10 (B lower panels). Cells were collected and analyzed for CSFE. Proportions of $CSFE^+$ cells with cell division were calculated as shown in the legend to Fig. 3. The representative data are shown. The similar results were obtained in separate three experiments.

incubated LCs, CSFE-labeled naïve $CD4^+$ T cells and splenic DCs in a trans-well system. When CSFE-labeled naïve $CD4^+$ T cells were incubated together with splenic DCs and the OVA peptide in an outer well, the $CD4^+$ T cells displayed extensive cell division in this cell culture system. In fact, the cell division percentage was 68% (Fig. 5A). Consistent with the above results, addition of LCs to the same well reduced it to 47% (Fig. 5B), and percent inhibition was 30.6%. In contrast, when LCs were added in an inner well separated by membrane that can translocate only soluble substances but completely not cells, the cell division percentage was not profoundly impaired (Fig. 5C). In fact, percent inhibition was 6.6%. These results clearly demonstrated that LCs require cell–cell contact with splenic DCs and/or naïve $CD4^+$ T cells to exert their inhibitory action.

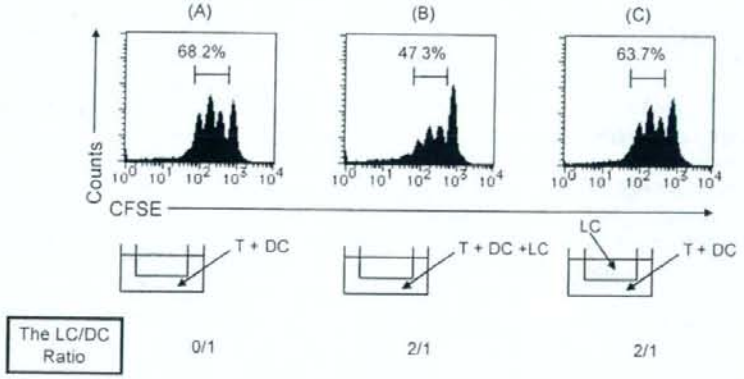

Fig. 5 Requirement of cell contact for LC regulation of naïve T cell activation CSFE-labeled naïve $CD4^+$ T cells prepared from DO11.10 mice were incubated with OVA peptide in the presence of splenic DCs (1 10^5 ml $^{-1}$) alone (A) or splenic DCs (1 10^5 ml $^{-1}$) plus LCs (2 10^5 ml $^{-1}$) (B) in a bottom well. The same cell number of LCs as shown in (B) were incubated in an upper well, and the other cells and the peptide were separately incubated in a bottom well (C). At day 3, cells were collected and analyzed for CSFE. Proportions of $CSFE^+$ cells with cell division were calculated. The representative data are shown. The similar results were obtained in separate three experiments.

4. Discussion

This is the first report clearly and formally demonstrating that freshly isolated LCs play a role as a negative regulator but entirely not an activator in the development of primary response to protein Ag in vitro. LCs have been regarded as professional APCs for mounting adaptive immune responses in the skin [3,4]. However, freshly isolated, highly purified epidermal LCs, although expressing comparable levels of MHC class II and costimulators as splenic DCs, did not activate naïve $CD4^+$ T cells (Figs. 1 and 2). Furthermore, LCs inhibited activation of naïve $CD4^+$ T cells induced by splenic DCs via cell-to-cell interactions (Figs. 3A and 5). However, this is not true for B cells although expressing $I\text{-}A^d$ and lacking naïve T cell activation (Figs. 1E and 3B), indicating that LCs uniquely exert active regulatory action on DC activation of naïve T cells. Thus, it is plausible that LCs might negatively regulate primary T cell responses in the skin.

Many investigators analyzed APC activity of LCs by using MHC class II-enriched epidermal cells post-incubation for several days in vitro [27,28]. However, there have been no reports on APC functions of freshly isolated LCs or on comparison study of APC functions between freshly isolated LCs and the LCs post-in vitro incubation. Microbial products can induce maturation of various types of DCs to become professional APCs with full capacity to activate naïve T cells [9]. For example, LPS, an agonist of TLR4, can activate bone marrow-derived DCs (BMDCs) and splenic DCs to produce various proinflammatory cytokines and to express higher levels of costimulators as well as MHC class II. However, LCs show poor responses upon LPS challenge despite expressing TLR4 [2]. These observations suggest that LCs might remain unchanged in terms of biological functions even during microbial infection in the skin and might persistently contribute to regulate the primary adaptive immune responses in the LNs draining the infectious sites of the skin.

Genetically LC-ablated mice were recently established by three different groups and provided us with new but controversial information on in vivo functions of LCs [1]. Knock-in mice that express diphtheria toxin receptors under the control of the langerin gene or the gene of its promoter exhibit absence of LCs in their epidermis when they were administered with diphtheria toxin or were crossed with transgenic mice over-expressing diphtheria toxin. These LC-ablated mice showed quite different phenotypes of CHS responses. They showed decreased, unchanged, or increased ear swelling upon cutaneous application with various haptens [3,13,15]. We do not know the exact reasons why the similarly manipulated mice exhibit quite different phenotypes. Nonetheless, adoptive transfer of LN cells from hapten-primed LC-ablated mice causes severer CHS response in naïve mice than those from hapten-primed wild-type mice, indicating the negative regulatory function of LC in the primary T cell responses [15]. Furthermore, mice topically applied with steroid showed exacerbated CHS response concomitant with numerically decreased LCs in their epidermis [29]. Our present results together with those reports might, at least partly, indicate the negative regulatory role of LCs in the primary T cell responses.

Accumulated lines of evidence have revealed functional and phenotypical heterogeneity of DCs [9]. In particular, mucosal immune system should play dual roles, a negative regulator of adaptive immune responses to prevent food allergy and an activator of adaptive immune responses to eliminate gut-invaded pathogens. To accomplish these opposite roles, mucosal immune system might carry functionally different DCs; regulatory DCs for the former and immunogenic DCs for the latter [9]. Some regulatory DCs in Peyer's patch produce IL-10 to negatively regulate the immune responses [23]. LCs might serve as a negative regulator by producing IL-10 as well. However, neutralizing anti-IL-10 did not inhibit the suppressive action of our freshly isolated LCs (Fig. 4B), indicating that IL-10 is not essential for the negative regulatory actions of LCs. Although TGF-b is reported to serve as negative regulator produced by DCs [8,10], neutralizing TGF-b could not restore the naïve T cell activation (Fig. 4A). Rather, cell-to-cell contact is required to achieve their negative regulatory functions (Fig. 5). The precise mechanisms underlying are unknown. It is also still to be elucidated which type of cells our LCs target, splenic DCs or naïve $CD4^+$ T cells. Further studies are needed.

Previous in vivo study revealed that administration of BMDCs matured by TNF-a and pulsed with thyroglobulin, an self-Ag responsible for autoimmune thyroiditis, inhibits the subsequent development of thyroglobulin-induced experimental thyroiditis by inducing IL-10-producing Tr1 cells specific for thyroglobulin [30]. These DCs may contribute to peripheral T cell tolerance. Furthermore, BMDCs prepared by the distinct protocol and loaded with OVA can evoke selective expansion of $CD25^+CD4^+$ Treg specific for OVA, a foreign Ag, in the draining LNs [31], suggesting involvement of those DCs in protecting allergic disorders. In these lines, LCs might initiate allergen- and/or auto-Ag-specific Treg. It is intriguingly to note that healthy volunteers exhibit rapid diminution of LCs in the skin, presumably due to their migration into the